Bunyamwera Orthobunyavirus Glycoprotein Precursor Is Processed by Cellular Signal Peptidase and Signal Peptide Peptidase

Xiaohong Shi[a1], Catherine H. Botting[b], Ping Li[a], Mark Niglas[b], Benjamin Brennan[a], Sally L. Shirran[b], Agnieszka M. Szemiel[a] and Richard M. Elliott[a2]

[a]MRC-University of Glasgow Centre for Virus Research, University of Glasgow, Glasgow G61 1QH, United Kingdom

[b]Biomedical Sciences Research Complex, University of St Andrews, St Andrews, KY16 9ST, United Kingdom

[1]To whom Correspondence should be addressed. Email: xiaohong.shi@glasgow.ac.uk

[2] This paper is dedicated to the memory of our colleague Richard M. Elliott who died on June 5 2015 whilst this work was ongoing.

Running title: Bunyamwera virus glycoprotein precursor processing

Author contributions: X.S., and R.M.E. designed research; X.S., P.L., M.N., B.B., and A.S. performed research; C.H.B., and S.L.S. performed MS; X.S. and R.M.E. wrote the Paper.

Significance

Bunyamwera virus (BUNV) is the prototype of the *Orthobunyavirus* genus and *Bunyaviridae* family that contains important human and animal pathogens. The cleavage mechanism of orthobunyavirus glycoprotein precursor (GPC) and the host proteases involved have not been clarified. Here we found that NSm and Gc contain their own internal signal peptides (SPs) which mediate the GPC cleavage by host signal peptidase (SPase) and signal peptide peptidase (SPP). Furthermore, the NSm domain-I (SP^{NSm}) plays an important post-cleavage role in cell fusion. Our data clarified the implication of host proteases in the processing of the orthobunyavirus GPC. This identifies SPP as a potential intervention target and the knowledge we gained will benefit the preventive strategies against other orthobunyavirus infections.

Abstract

The M genome segment of Bunyamwera virus (BUNV), the prototype of both the *Bunyaviridae* family and the *Orthobunyavirus* genus, encodes the glycoprotein precursor (GPC) that is proteolytically cleaved to yield two structural glycoproteins, Gn and Gc, and a nonstructural protein NSm. The cleavage mechanism of orthobunyavirus GPCs and the host proteases involved have not been clarified. In this study, we investigated the processing of BUNV GPC and found that both NSm and Gc proteins were cleaved at their own internal signal peptides (SPs), in which NSm domain-I functions as SP^{NSm} and NSm domain-V as SP^{Gc}. Moreover, the domain-I was further processed by a host intramembrane-cleaving protease, signal peptide peptidase (SPP) and is required for cell fusion activities. Meanwhile, the NSm domain-V (SP^{Gc}) remains integral to NSm, rendering the NSm topology as a two-membrane-spanning integral membrane protein. We defined the cleavage sites and boundaries between the processed proteins: Gn, from residue 17 to 312 or nearby residues; NSm, 332 to 477; and Gc, 478 to 1432. Our data clarified the mechanism of the precursor cleavage process, which is important for our understanding of viral glycoprotein biogenesis in the genus *Orthobunyavirus* and thus presents a useful target for intervention strategies.

\body

The family *Bunyaviridae* contains more than 350 named viruses that are classified into the five genera *Orthobunyavirus*, *Hantavirus*, *Nairovirus, Phlebovirus, and Tospovirus*, making it one of the largest families of RNA viruses. Several members of the family are serious human pathogens, such as La Crosse virus (LACV) and Oropouche virus (OROV) (*Orthobunyavirus*), Hantaan (HTNV) and Sin Nombre viruses (*Hantavirus*), Rift Valley fever virus (RVFV)

54 *Phlebovirus*) and severe fever with thrombocytopenia syndrome Virus (SFTSV) (*Phlebovirus*),
55 Crimean-Congo hemorrhagic fever virus (CCHFV, *Nairovirus*) (1, 2). The characteristic
56 features of bunyaviruses include a tripartite single-stranded RNA genome of negative- or
57 ambi-sense polarity, cytoplasmic site of viral replication, and assembly and budding at
58 membranes of the Golgi complex (1-3). Bunyamwera virus (BUNV), the prototype of both
59 the family and the *Orthobunyavirus* genus, remains an important research model for many
60 pathogens within this family.

61 The medium (M) genomic RNA segment of orthobunyaviruses encodes the glycoprotein
62 precursor (GPC; in order Gn-NSm-Gc) that is cotranslationally cleaved to yield the mature
63 viral glycoproteins Gn and Gc, and a nonstructural protein NSm. Gn and Gc form viral spikes
64 that play a crucial role in virus entry (1, 2). Both Gn and Gc are type I integral
65 transmembrane proteins and form a heterodimer in the endoplasmic reticulum (ER) prior to
66 trafficking to, and retention in, the Golgi compartment where virus assembly occurs (2, 4,
67 5). Bunyavirus glycoproteins are fusogenic and the fusion peptide is located on Gc, a class II
68 fusion protein (6), but cell fusion requires the co-expression of both Gn and Gc
69 glycoproteins (7). NSm, an integral membrane protein, comprises three hydrophobic
70 domains (I, III and V) and two non-hydrophobic domains (II and IV) (Fig. S1*A*) and its N-
71 terminal domain (I) is required for BUNV replication (8).

72 Cleavage of BUNV GPC is mediated by host proteases, but the details of which
73 proteases are involved and the precise cleavage sites have not been clarified. Experimental
74 data on GPC processing has only been reported for snowshoe hare orthobunyavirus (SSHV);
75 the carboxyl terminus of SSHV Gn was determined by C-terminal amino acid sequencing to
76 be an arginine (R) residue at position 299 (9) (Fig. S1*B*). Based on alignments of several
77 orthobunyavirus GPC sequences, it was suggested that Gn-NSm cleavage occurs at a similar
78 position to that defined for SSHV (10). This arginine (302R for BUNV) appears conserved in

GPCs of all orthobunyaviruses analyzed to date, and for most of the viruses lies in the sequence R-V/A-A-R (Fig. S1*C*), which has been believed as the site of Gn-NSm cleavage by furin-like proteases (11).

In eukaryotes, most secreted and membrane proteins contain cleavable N-terminal signal peptides (SPs), which are recognized by the signal recognition particles (SRP) when nascent polypeptide chains emerged from the ribosome at ER and translocate it into the ER lumen where they are usually cleaved by cellular signal peptidases (SPase) (12). The imbedded peptide remnant is usually subsequently released for degradation by the cellular signal peptide peptidase (SPP) or SPP-like proteases, which belong to the family of intramembrane-cleaving aspartyl proteases (I-CliPs) (13-16). SPP is an ER-resident I-CliPs (17) and is implicated in other important biological functions, such as in generating C-terminal peptides for MHC class I presentation (18) and human lymphocyte antigen E (HLA-E) epitopes (19). SPP activities also involve in the intra-membrane cleavage of the core proteins of hepatitis C virus (HCV), GB virus B and classical swine fever virus (CSFV) (family *Flaviviridae*) (20, 21).

To investigate the cleavage events of orthobunyavirus GPC, we used several approaches including mutagenesis, virus assays, RNA interference, mass spectrometry and biological assays. We aimed to determine the cleavage sites between the boundaries of the mature proteins, e.g. Gn and NSm, and NSm and Gc. Our data revealed the implementation of the cellular SPase and SPP in the cleavage of BUNV GPC and clarified the mechanism of orthobunyaviruses GPC cleavage.

Results

Gn-NSm Cleavage Does Not Occur at the RVAR Motif by Furin-like Proteases. We first investigated whether the Gn-NSm cleavage takes place between residues 302R and 303R at the RVAR motif (Fig. S1). Five mutations were generated at this site in the M expression plasmid pTM1BUNM, including a deletion mutation (ΔRVAR) and four substitution mutations (MMKR, AAAA, RSLK and RRKR) (Fig. 1*A*). These plasmids were transfected into BSR-T7/5 cells and the radiolabeled viral proteins were immunoprecipitated with anti-BUN serum followed by SDS-PAGE fractionation. Interestingly, like the wild-type (wt) BUNM control, all mutated GPCs were cleaved into Gn, NSm and Gc (Fig. 1*B*), suggesting this location is not a cleavage site by furin-like proteases. Furthermore, the furin inhibitor I (dec-RVKR-cmk, Calbiochem) had no effect on the BUNV GPC cleavage (Fig. S2*A*) and yields of virus produced in the presence of the drug over 30 hrs (Fig. S2*B*).

There exist eight residues between residues 302R and 311S at Gn-NSm junction (Fig. S1 *and* Fig. 1*C*). To investigate whether these residues harbor the Gn-NSm cleavage site, we constructed six mutants that contain internal progressive deletions between residues 298L and 311S (Fig. 1*C*). As shown in Fig 1*D*, all mutated precursors were properly cleaved. Moreover, the deletions resulted in the increased migration of Gn bands on the gel, with a relative shift corresponding to the number of amino acids removed (lanes 3 to 8), suggesting that these residues still belong to the Gn cytoplasmic tail (Gn CT) and the Gn-NSm cleavage must occur at or within NSm domain-I.

NSm Domain-I Functions as an Internal Signal Peptide. After excluding the Gn-NSm cleavage at motif $RVAR^{302}$, we speculated that NSm domain-I, a type II transmembrane domain (TMD), could function as an internal SP for NSm (SP^{NSm}). Using SignalP 4.1 server (www.cbs.dtu.dk/services/SignalP/) (22) the domain was predicted as a cleavable internal

125 SP that cleaves between residues 331G and 332T (Fig. S3*A* and Fig.2*A*). It has been reported
126 that the residues at the -3 and -1 positions relative to the SPase cleavage site are most
127 critical for cleavage by cellular SPase complex (23). Therefore, we generated a series of
128 mutant GPCs, including six substitution mutations at the -3 and -1 positions and one
129 substitution mutation in the core region of the domain (SPm) (Fig. 2*A*). When the residues
130 at either -3 (329I) or -1 (331G), or at both positions, were changed to the charged arginine
131 (R), the NSm protein was not detected (Fig. 2*B*, lanes 2, 4 and 6). However, substitution with
132 alanine at these positions and substitution mutation within the domain (SPm) did not affect
133 Gn-NSm cleavage (lanes 3, 5, 7 and 8) in that NSm was clearly seen. Furthermore, we
134 purified NSm protein from the cells infected with recombinant virus, rBUNNSmV5, in which
135 the V5-epitope was inserted in the NSm cytoplasmic domain (Fig. S3*B*), for mass
136 spectrometric (MS) analysis and confirmed that the residue 332T is the first N-terminal
137 residues of NSm (Fig. S3*C* and S3*D*).

138 The effects of the mutations on glycoprotein function were also assessed with regard to
139 the Golgi trafficking and cell fusion activities. Consistent with the above observation, the
140 arginine substitutions at -3 and -1 position totally abolished Golgi targeting (Fig. 2*C*, panels
141 *c*, *e*, and *g*) and cell fusion (panels *d*, *f* and *h*), whereas alanine substitution had no effect on
142 either Golgi colocalization (panels *l*, *o* and *r*) or cell fusion (panels *m*, *p* and *s*). When these
143 mutations were tested for virus rescue, we were able to generate viruses from M segment
144 mutants containing alanine substitution mutations (rAEG, rIEA and rAEA), but not from
145 arginine substitution mutants. The rescued viruses showed similar plaque phenotypes to
146 the wt control (panels *n*, *q* and *t*). Taken together, our data confirmed that the NSm
147 domain-I functions as an internal SP^{NSm}.

148 **Mapping the C-termini of Gn Protein.** After SPase cleavage of SP^{NSm} at residue 332T,
149 the SP is still attached to the upstream Gn CT (preGn). To define the Gn end, we constructed

150 a series of individual Gn mutants that terminate between residues 298 to 332 (Fig. 3*A*).
151 Consistent with the earlier results from internal deletions, the deletions from residues 312
152 to 298 resulted in the linear reduction in the molecular weight of Gn proteins (Fig. 3*B*, lanes
153 4 to 7) and Gn312 is comparable in size to wt Gn (comparing lanes 3 and 7), indicating that
154 Gn likely ends at residue 312 or nearby residues. However, deletions in SP^{NSm} did not cause
155 a linear reduction in Gn molecular weights (lanes 8 to 10). It is noticeable that Gn317, which
156 contains only five remnant hydrophobic residues at the C-terminus, produced a smaller
157 band (about 25 kDa), which we believed to be a degradation product (lane 8). We also
158 compared the size of the intracellular and virion Gn proteins and found no difference (Fig.
159 3*C*), confirming the intracellular and virion Gn proteins end at same position.

160 To confirm the subsequent processing of SP^{NSm} upon SPase cleavage, we constructed a
161 mutated Gn (Gn308V5) with domain-I replaced with non-hydrophobic V5 epitope and a
162 further 6 residues from the Gc CT (QEIKQK) (Fig. 3*A*). It is worth mentioning that the
163 unprocessed Gn332 (preGn) would be similar in size to Gn308V5 (35.33 v 35.12 kDa). As
164 anticipated, Gn308V5 runs at a higher molecular weight than wt Gn and the processed
165 Gn332 (Fig. 3*D*), indicating that SP^{NSm} was further processed from preGn. The preGn was
166 visible by Western blot (WB) analysis of V5-tagged Gn proteins (Gn-27V5 and Gn-86V5) as a
167 faint band above the predominant processed Gn protein (Fig. 3*E*). Cell fusion assays with Gn
168 mutants (in co-expression with Gc) indicated that the extensive syncytia were formed only
169 from cells coexpressing Gc and Gn332 (PreGn), and any deletions in SP^{NSm} diminished the
170 cell fusion (Fig 3*F*), suggesting that the liberated SP^{NSm} is required in cell fusion.

171 MS analysis of virion Gn protein identified 17S as the first residue of the processed Gn
172 protein (Fig. S4*B*), but unable to confirm the Gn end, with the furthest C-terminal residue
173 was mapped to 303R (Fig. S4*C* and SI Table), similar to the previously determined SSHV Gn
174 end (9). It is probably due to the fact that the newly identified Gn C-terminal residues (303

to 312) is rich in positively charged arginine and lysine residues being targets by trypsin-like proteases (24). The terminal residues identified by MS are summarized in Table S1.

NSm domain-V functions as an internal noncleavable SP^{Gc}. Our previous study suggested that NSm domain-V functions as a SP^{Gc} (8). Indeed, the deletion of the domain abolished Gc processing as no Gc protein was detected from the mutated BUNV GPCs that contain whole or partial internal deletion in the domain (Fig. 4*A*, lanes 4 to 6). To study whether the domain undergoes any further processing as SP^{NSm}, we compared the size of C-terminal truncated NSm proteins (based on pTmBUNGn-NSmV5) (Fig. 4*B*). The deletions resulted in the increased migration shift of NSm bands (Fig. 4*C*, lanes 4 to 8). NSm476 that contains the intact domain-V was identical in size with the parental NSmV5 (comparing lanes 9 and 10), indicating that domain-V is not further cleaved. Furthermore, no size change was noticeable when the domain-V was swapped by either non-hydrophobic residues from EGFP (residues 1 to 20) or hydrophobic signal peptide of Hantaan virus (HTNV, strain 76-118) Gn protein (SP^{HGn}, residues 1 to 19) (Fig. 4*D*), whereas NSm456 that lacks the domain-V was obviously smaller (Fig. 4*D*, lane 6), providing corroborating evidence that SP^{Gc} remains integral to the mature NSm. This renders the topology of mature NSm as a two-membrane-spanning protein (residues 332 to 477) that consists of the ectodomain (II), TMD (III), endoplasmic loop (IV) and C-terminal type-II TMD (V) (Fig.4*E*).

Requirement of SP^{NSm} for Cell Fusion and Virus Replication. To further investigate the role of SP^{NSm} in virus replication, we made four mutant GPC constructs (Fig. 5*A*), and compared the impact of mutations in promoting cell fusion and virus viability. All four mutated GPCs were cleaved into Gn and Gc, and also NSm from the BUNM-SPm^{NSm} and -SP^{NSm}/HTNtm (Fig. 5*B*). A cell fusion assay revealed that only the GPC-ΔNSm_I, which contained deletion of whole mature NSm (residues 332 to 477) but retained SP^{NSm} for Gc translocation, produced extensive syncytial formation (Fig. 5*C*). For other three GPC mutants, the domain-V, SPm^{NSm},

and SP^{NSm}/HTNtm functioned properly as SP^{Gc} for GPC processing, but these mutated GPCs failed to cause cell fusion. Consistently, from GPC-ΔNSm_I we rescued a recombinant virus (rBUNΔNSm) that did not express NSm protein (Fig. 5*D*, lane 4). The rBUNΔNSm was attenuated, evidenced by smaller plaque phenotype (Fig. 5*E*) and reduced virus yield at late infection (Fig. 5*F*). As BUNV NSm is one of key factors in the Golgi associated "virus factory", the depletion of the protein likely affects the virus assembly (8, 25, 26). The same strategy was used to create a viable recombinant OROV lacking NSm (27).

To characterize further SP^{NSm}, we assessed the effect of the deletion mutations in the domain on GPC processing and cell fusion. As we mentioned early, deletions in SP^{NSm} did not lead to a linear reduction in the molecular weight of Gn proteins (Fig. 5*G*). The Gn bands from Gn324 to Gn332 are comparable in size with wt Gn (lanes 6 to 11), but further deletion towards Gn312 (in the case of Gn317 and Gn322) would interrupt the proper processing of Gn protein (lanes 4 and 5), suggesting that the processing requires the stable SP TMD structure. When these mutants were tested in cell fusion, we noticed that even removal of two residues from SP^{NSm} (Gn330) had a significant impact on syncytia formation and that further deletions diminished the extent of cell fusion (Fig. 5*H*). The data together indicated that in addition to the role as SP, the liberated SP^{NSm} has post-cleavage function.

Involvement of SPP in the Processing of BUNV GPC. As SPP is the ER-resident I-Clips, we suspect that SPP is probably involved in the further processing of SP^{NSm}. To address the issue, we generated three lentiviruses that express small hairpin RNAs (shRNAs): two specific to human SPP mRNA and one to EGFP (shGFP) as negative control. Both shSPP1 and shSPP2 were able to inhibit the SPP expression in the transduced A549 cells (shSPP2 showed a better silencing effect) (Fig. 6*A*). We then examined the impact of SPP knockdown on BUNV replication following low multiplicity infection of A549V cells (MOI of 0.01 pfu/cell). WB analysis showed that the detection of BUNV N was delayed by 24 hrs in shSPP-silenced

cells compared with shGFP control (Fig. 6*B*) and the virus titre in SPP-knockdown cells was over 10-fold lower than controls across the infection period (Fig, 6*C*). This indicates the likely involvement of SPP in BUNV replication. In order to investigate if SPP is implicated in replication of other bunyaviruses, we infected the transduced A549V cells with SBV (*Orthobunyavirus* genus), RVFV (*Phlebovirus* genus) and Puumala virus (PUUV, *Hantavirus* genus), and their N proteins and virus titres were determined by WB and plaque assay. A significant inhibitory effect of SPP silencing was observed for SBV (Fig. 6*D* and 6*E*). For RVFV, Inhibition was noticeable but to lesser extent than BUNV and SBV (not statistically significant) (Fig. 6*F* and 6*G*). Significant inhibition of PUUV replication was observed for PUUV replication in SPP-knockdown cells (Fig. 6*H* and 6*I*), but PUUV growth was inhibited to a great extent in shGFP control cells than in SPP-knockdown cells, evidenced by the N protein detection in SPP-knockdown cells but not in shGFP control at 72 hrs p.i. (Fig. 6*H*, lane 7 at bottom panel of long exposure) and significantly lower virus titre in shGFP control (Fig, 6*I*). This pattern for PUUV is largely due to antiviral activity we found present in shGFP lentivirus preparation (Fig. S5*A*), to which PUUV is more sensitive to the inhibitory effect on virus replication than BUNV to the inhibition effect (Fig. S5*B*).

The inhibitory effect of SPP knockdown on BUNV infection was also visualized using a recombinant virus (rBUNGc-eGFP) with eGFP fused to Gc (3). Naïve Huh7 cells and cells expressing shSPP2 were infected with rBUNGc-eGFP (MOI of 0.01), and cells were examined at 10, 24 and 48 hrs p.i. by fluorescence microscopy. Production of eGFP-tagged Gc, and hence production of progeny virus particles, was observed in naïve cells at 10 hrs p.i. and virus spread to adjacent cells was clearly evident at 24 hrs p.i. All cells were infected by 48 hrs p.i. (Fig 6*J*, panels a to c). In SPP-knockdown cells, the eGFP-tagged Gc was not observed until 24 hrs p.i., and the spreading to neighboring cells was still limited at 48 hrs p.i. (panels d to f).

Discussion

The cleavage between BUNV Gn and NSm has long been thought to occur at the amino acid motif RV/AAR, which is conserved in several orthobunyaviruses (10, 11) and fits the minimum furin cleavage site (RXXR)(28). However, as the furin-like proprotein convertases (PCs) process substrates in the lumen of the Golgi complex and endosome or at the cell surface (29), it is unlikely that the RxxR motif in the Gn CT can be accessed by these proteases. Moreover, some members of the genus *Orthobunyavirus*, such as Wyeomyia virus (WYOV), SBV and OROV lack the RxxR motif (Fig. S1*C*). In fact, we have proven that the motif and the downstream eight residues (residues 303 to 310) are still part of Gn CT. In the *Bunyaviridae* family, the furin-like protease is involved in the GPC processing of CCHFV (*Nairovirus* genus) for generating a 38-kDa NSm protein, whereas the CCHFV furin site is located at the ectodomain of pre-Gn protein (30).

By using mutagenesis and MS analysis we confirmed that the NSm domain-I is SP^{NSm} which is cleaved by SPase at residue 332T of mature NSm. The residual SP^{NSm}, which is still linked to the upstream Gn CT (as preGn), is further processed from Gn C-terminus by the ER-resident SPP. The implication of SPP in BUNV GPC process is validated by our observations: 1) The further processing of NSm domain-I (SP^{NSm}) upon SPase cleavage, 2) the detection of preGn by WB analysis of V5-tagged Gn protein, and 3) Inhibition of BUNV and SBV infection in SPP-knockdown cells. We also assessed the impact of SPP knockdown on two other bunyaviruses, RVFV (*Phlebovirus*) and PUUV (*Hantavirus*). SPP knockdown had no significant inhibitory effect on RVFV infection, whereas it inhibited PUUV infection. However, as PUUV replicated less efficiently in the shGFP-induced cells, we were unable to draw a clear conclusion. Some lentivirus expressing shRNAs can trigger IFN activation(31) and the effect of siRNA on innate immunity is sequence and structure related (32). It should

be mentioned that the coding strategies and sizes of products encoded by M segments of the viruses in the family are very divergent and thus it is plausible that the precursor processing differs from genus to genus.

Besides its role as a SP, we provide evidence that the liberated SP^{NSm} has post-cleavage function in cell fusion. We speculate that the liberated SP^{NSm} is likely incorporated into the virion by interacting with one of viral glycoproteins upon cleavage by SPP, which is probably required for that interaction. However, we were unable to find the peptide from the purified virus particles by MS analyses, perhaps due to the technical challenge for the reason of the small size and hydrophobicity of the domain. Another possibility is that the Gn CT is modified during the processing of SP^{NSm} by SPP and that modification might be crucial for glycoprotein activities. Whatever the cases, it seems that the sequence specificity of SP^{NSm} is important. Several signal peptides of viral proteins have post-cleavage functions. For instance, $SP^{GP\text{-}C}$ of lymphocytic choriomeningitis virus and Junín virus (Arenaviruses) precursor glycoproteins C (GP-C) is an essential structural component of mature virions and is required in both glycoprotein maturation, cell fusion and virus infectivity (33-35).

Based on our findings, we propose a new model for the process and topology of orthobunyavirus glycoproteins (Fig. 7*A*). All three proteins, in precursor form, contain their own SPs. The N-terminal SP^{Gn} targets the nascent Gn polypeptide through the ER membrane where it is cleaved by SPase at residue 17S. The internal SP^{NSm} mediates the translocation of the nascent NSm chain into the ER membrane and it is subsequently cleaved at residue 332T by SPase from the NSm. SP^{NSm} is further processed by SPP to free the Gn CT. NSm domain-V/SP^{Gc} translocates the nascent Gc chain to the ER membrane and is cleaved at residue 478E to separate the mature NSm and the nascent Gc chain. However, unlike SP^{NSm}, the domain-V/SP^{Gc} is not further processed and remains as the C-terminal domain of mature NSm. The new topology model of mature Gn, NSm and Gc proteins is illuminated in Fig. 7*B*.

Gn and Gc proteins are type I transmembrane proteins and NSm is a two-membrane-spanning protein.

This study revealed a new dimension for SPP in virus replication. The new knowledge will benefit vaccine development and help identify new antiviral drugs against pathogenic virus infections caused by viruses in the family. Indeed, with the knowledge we gained we have generated recombinant BUNV and SBV viruses that lack full mature NSm as well as NSs proteins (Shi; et al., unpublished data) and these viruses would be potential candidates or tools for vaccine development.

Materials and Methods

The materials and methods are described in *SI Materials and Methods.* They include antibodies, plasmids and mutagenesis, transfection of cells, metabolic radiolabeling and immuno-precipitation, immunofluorescence staining, BUNV glycoprotein fusion assay, virus rescue by reverse genetics, virus infection, titration and purification, preparation of BUNV glycoprotein Gn, Gc and NSm proteins, mass spectrometric (MS) Analysis, SPP knockdown by lentivirus shRNA, western blotting (WB).

Cells and Viruses. A549, A459V (36), A549-NPro (37), Vero E6, BHK-21, HEK 293T, Huh7 and BSR-T7/5 (38) cells were maintained as described previously (4). BUNV, SBV, RVFV (strain MP12) and Puumala virus (PUUV, strain CG1820) were used as representative strains for genera of *Orthobunyavirus, Phlebovirus and Hantavirus* in SPP knockdown assays. rBUNGc-eGFP is a recombinant BUNV with the truncated Gc tagged by eGFP (3).

Statistical Analysis. Data were expressed as the mean and SD. The *P* value and statistical significance of difference was analyzed by using unpaired *t* test with GraphPad 6 software. **P* value < 0.05, significant; ***P*< 0.01, very significant; ****P* <0.001, extremely significant.

ACKNOWLEDGEMENTS

We thank Drs. Klaus K. Conzelmann (Ludwig-Maximilians-Universität München), David Jackson and Richard Randall (University of St. Andrews) and Martin Lowe (University of Manchester) for providing reagents used in this work, Drs. Friedemann Weber (Justus-Liebig-Universität Gießen) and Alain Kohl (University of Glasgow) for critical reading of the manuscript. We also thank Angela Elliott and Edward Dornan and Dr. Ye Liu for technical support. This study was supported by Wellcome Trust grant (to RME) and grant (094476/Z/10/Z) that funded the purchase of the TripleTOF 5600 mass spectrometer at the BSRC of University of St Andrews.

Figure Legend

Fig. 1. Gn-NSm does not cleave at the previously predicted RVAR site. (*A*) Substitution and internal deletions at RVAR motif. (*B*) Effect of deletion and substitution mutations on GPC cleavage. (*C*) Internal deletions between residues 298L and 311S at Gn-NSm junction. (*D*) The processing of mutant GPCs. Transfected BSRT7/5 cells were radiolabeled with [35S]methionine. The viral proteins were immunoprecipitated with anti-BUN and analyzed by SDS-PAGE. The position of the viral proteins is marked.

Fig. 2. NSm domain-I acts as an internal SP^{NSm}. (*A*) Mutations at -3 (329I) and -1 (331G) positions of the SPase cleavage site (on pTM1-BUNM-NSmV5). (*B*) Effect of substitution

mutations on NSm processing. The radiolabeled viral proteins were immunoprecipitated with anti-V5 antibody. (*C*) Effect of mutations on the Golgi targeting of the viral glycoproteins, cell fusion and virus viability. For immunofluorescence assays, the transfected BSRT7/5 cells were stained with a mixture of anti-Gc MAb (M810, in red) and anti-GM130 (in green for the Golgi staining) antibodies and examined by confocal microscopy. Nuclei were stained in blue with DAPI. Cell fusion and virus rescue were performed as described in SI Materials and Methods.

Fig. 3. Mapping the C-termini of Gn protein by mutagenesis. (*A*) Mutations in the Gn CT and NSm domain-I (on pTM1BUN-Gn332). '*' represents the stop codon. (*B*) Effect of deletions on the migration shift of Gn protein. (*C*) Profile of the radiolabeled intracellular and virion proteins. (*D*) The expression of Gn332 (preGn) and Gn308V5. (*E*) Western blot (WB) analysis of V5-tagged Gn332 at residue 27 or 86. (*F*) Cell fusion assay on BSRT7/5 cells co-transfected with pTM1BUN-NSmGc (Gc) and one of the Gn mutants.

Fig. 4. NSm domain-V functions as a noncleavable SP^{Gc}. (*A*) Deletion of Domain-V abolished the Gc processing. (*B*) Mutations at NSm domain-V. '*' represents the stop codon. (*C*) Effect of deletions on the migration shift of the V5-tagged NSm protein. (*D*) WB analysis of V5-tagged NSm and its mutants. (*E*) The revised topology of NSm protein.

Fig. 5. Requirement of SP^{NSm} for GPC processing, cell fusion and virus replication. (*A*) Schematic showing either deletion of NSm or mutations in SP^{NSm}. (*B*) Effect of mutations on the GPC cleavage. (*C*) Cell fusion on BSRT7/5 cells transfected with BUNM mutants. (*D*, *E* and *F*) The protein profile (*D*), plaque phenotype (*E*) and growth curve (*F*) of the recombinant virus lacking NSm (rBUNΔNSm). (*G*) Effect of deletion mutations in SP^{NSm} on the migration shift of Gn protein. (*H*) Cell fusion on BSRT7/5 cells co-transfected with pTM1BUN-NSmGc and one of the Gn mutants.

Fig 6. SPP KO affects BUNV infection. (*A)* SPP-knockdown in A549 cells. (*B* and *C*) WB analysis (*B*) and Growth kinetics (*C*) of BUNV infection in shRNA expressing A549V cells. (*D* and *E*) Effects of SPP-knockdown on SBV infection. (*F* and *G*) Effects of SPP knockdown on RVFV infection. (*H* and *I*) Effects of SPP-knockdown on Puumala virus (PUUV) infection. The transduced A459V cells were infected with virus (MOI of 0.01). At each time point the supernatants were harvested for virus titration and cell lysates were collected for WB. The relevant proteins were probed with antibodies against SPP, tubulin (T) or viral N proteins. (*J*) Effect of SPP-knockdown on BUNV spreading. Transduced Huh7 cells were infected with rBUNGc-eGFP (MOI of 0.01) and incubated until time points (10, 24 and 48 hrs p.i.) as indicated. Cells were stained with anti-GM130 and examined by confocal microscopy. EGFP-tagged Gc and virus particles were shown in green, GM130 were stained in red and the nuclei were stained in blue with DAPI.

Fig. 7. The model of BUNV GPC (Gn-NSm-Gc) cleavage. (*A*) Schematic showing BUNV GPC processing. (*B*) Topology of Gn, Gc and NSm proteins. See discussion for details.

Supporting Information

SI Materials and Methods

Antibodies. MAb810, a monoclonal antibody against BUNV Gc, anti-BUN and anti-NSm, the rabbit antisera against BUNV particles and NSm peptide TDQKYTLDEIADVLQA (residues 338 to 353 of BUNV GPC), have been described previously (26). Rabbit anti-BUN N, anti-SBV N and anti-RVFV N antisera were raised against nucleoproteins of BUNV, SBV and RVFV, respectively(39-41). A rabbit antiserum against GM130, a cis-Golgi matrix protein was provided by Dr M. Lowe (University of Manchester, UK). Other antibodies were purchased commercially: rabbit polyclonal antibody against SPP (anti-SPP) (Abcam); mouse monoclonal antibody against the V5 epitope (anti-V5) (Serotec); goat anti-rabbit antibody conjugated with fluorescein isothiocyanate (FITC) (Sigma), and goat anti-mouse antibody conjugated with Cy5 (Chemicon International Inc).

Production of Anti-PUU N. The 6His-tagged Puumala virus (PUUV) N protein was expressed in BL21-CodonPlus (DE3)-RP *E. coli* (Agilent Technologies) under IPTG induction at 18-20 °C for 20 hrs, purified with Ni–NTA resin and its identity confirmed by mass spectrometry. The purified PUU N was used for generating rabbit antisera against PUUV N protein (Eurogentec).

Plasmids and Mutagenesis. Plasmids that generate full-length BUNV antigenome RNA transcripts, pT7riboBUNL(+), TVT7R-BUNM(+), and pT7riboBUNS(+), or express the full length GPC, pTM1-BUNM, have been described previously (8, 42); pT7riboBUNM-NSmV5(+) and pTM1BUNM-NSmV5 contain the V5 epitope (GKPIPNPLLGLDST) inserted between residues 403 and 420 of the NSm coding region (Fig. S3*B*). The substitution and internal deletion mutations in BUNV GPC (in the backbone of either pTM1-BUNM for high

expression or pT7riboBUNM for virus rescue) were generated by PCR-directed mutagenesis on the appropriate parental templates.

A series of individual Gn expression plasmids (pTM1BUNGn298 to Gn332) were derived from pTM1BUNM (Fig. 3*A*) and Gn-NSm expression plasmids (pTM1BUNGn-NSmV5-454 to 476) were derived from pTM1BUNM-NSmV5 (Fig. 4*A*), in which the V5 epitope is inserted in the NSm cytoplasmic domain (IV) between residues 403 and 420 (Fig. S4*B*). The V5 tagged NSm was also introduced into TVT7RBUNM[+] for generating recombinant virus containing V5-tagged NSm. Two mutated Gn-NSm constructs (pTmBUNGnNSmV5-SP^{Gc}/SP^{HGn} and pTmBUNGnNSmV5-SP^{Gc}/$eGFP_{1\text{-}20}$) were created by replacement of the domain-V with either signal peptide of Hantaan virus Gn protein (residues 1 to 19) or N-terminal 20 residues of eGFP (Fig. 4A). Three mutated GPC constructs (pTM1BUNMΔ446-476, Δ457-476 and Δ467-476) contain internal deletions in the coding region of NSm domain IV and V). pTM1BUN-NSmGc expresses NSm and Gc proteins (residues 309 to 1433). pTmBUNMΔNSm_V and pTmBUNMΔNSm_I contain internal deletions in NSm coding region, in which ΔNSm_V has deletion of NSm domains I to IV (residues 311 to 456) except domain-V (SP^{Gc}) and pTmBUNMΔNSm_I has deletion of NSm domains II to V (residues 332 to 477) except domain-I (SP^{NSm}) as SP for Gc. pTMBUNM-SP^{NSm}/HTNtm has 17 residues of SP^{NSm} (residues 311 to 327) swapped with those of HTNV Gn TMD (TFCFGWVLIPAITFIIL, residues 490 to 506) (Fig. 5A). pTmBUNM-SPm^{NSm} contains four point mutations in the coding region of NSm domain-I (Fig. 2*A*). All the constructs were confirmed by DNA sequencing.

Transfection of Cells. BSRT7/5 cells were grown either in 35-mm dishes for immunoprecipitation experiments or in 12-well plate for cell fusion assay, or on 13-mm glass coverslips for immunofluorescence assays. Cells were transfected with the mixtures of plasmid DNA and transfection reagent (Lipofectamine® 2000 Transfection Reagent, Invitrogen) and incubated at 37°C for 24 hrs.

Metabolic Radiolabeling and Immunoprecipitation. At 24 hrs post transfection or post infection (p.i.), cells were labeled with [35S]methionine (PerkinElmer) for 3 hrs. For labelling of virus particles, the infected BHK21 cells grown in 175-cm2 flask were labelled with [35S]methionine for 6 hrs p.i. and virus particles were purified by ultracentrifugation (4). Cells were then lysed on ice in 300 µl of non-denaturing RIPA buffer (50 mM Tris-HCl [pH7.4], 1% Triton X-100, 300 mM NaCl, 5 mM EDTA) containing a cocktail of cOmplete protease inhibitors (Roche). BUNV proteins were immunoprecipitated with anti-BUN, anti-NSm or anti-V5 antibodies conjugated to Dynabeads Protein A (Novex, Life Technologies). The beads bound to immune complexes were washed with RIPA buffer containing 0.1% Triton X-100 and with cold PBS, and bound viral proteins were analyzed by SDS-PAGE under reducing conditions.

Immunofluorescence Staining. The transfected or infected cells were fixed with 4% formaldehyde-2% Sucrose-PBS and permeabilized with 0.2 % Triton X-100 in PBS before staining with specific primary antibodies and secondary antibody conjugates. Cells were examined using a Zeiss LSM confocal microscope.

BUNV Glycoprotein Fusion Assay. BSR-T7/5 cells, grown on 12-well plates, were transfected with 1 µg of either pTM1-BUNM or one of the mutant M expression plasmids. At 24 hrs post transfection, cells were treated with low pH medium (pH 5.3) for 15 min and then the medium was replaced by GMEM supplemented with 10% foetal calf serum (FCS). After incubation for 4 hrs at 37 °C the extent of cell fusion was observed following Giemsa staining. Cells that contain more than 3 nuclei are considered as syncytia and the nuclei in 30 syncytia in total were counted. The fusion is represented as average nuclei per syncytium (n = 30).

Virus Rescue by Reverse Genetics. Rescue experiments were performed essentially as described previously with minor modifications (42). Sub-confluent monolayers of BSR-

458 T7/5 cells grown in T25 were transfected with a mixture of plasmids comprising 1.0 μg each
459 of pT7riboBUNL(+), pT7riboBUNS(+) and TVT7RBUNM(+) or one of the M cDNA mutants,
460 and 7.5 μl Lipofectamine 2000 (Life Technologies) in 0.7 ml Opti-MEM media (Life
461 Technologies). At 4 hrs post transfection, 4 ml growth medium was added and incubation
462 continued at 33°C until CPE was evident.

463 **Virus Infection, Titration and Purification.** Cells seeded in dishes or flasks were
464 infected at an MOI of 0.01 or 1.0 PFU/cell. The inoculum was removed after 1hrs, and cells
465 were washed with PBS to remove the unattached viruses. Supernatants were harvested at
466 the indicated time points. BUNV and SBV were titrated by plaque assay on BSRT7/5 cells
467 and RVFV on BHK21 cells. The PUUV was titrated on Vero E6 cells by using the Avicel
468 immunofocus assay. Briefly, the virus infected cells were covered with 0.6% Avicel (FMC
469 BioPolymer) overlay medium and incubated for 7 days, fixed with 4% formaldehyde-PBS and
470 permeabilized with 0.5% Triton-100, 20mM glycine-PBS. Cell monolayer was blocked with 4%
471 skimmed milk, reacted with anti-PUUN and probed with peroxidase-conjugated anti-rabbit
472 IgG. The foci were developed after incubation with True Blue peroxidase substrate (KPL).
473 The purification of BUNV particles was described previously (4).

474 **Preparation of BUNV Glycoprotein Gn, Gc and NSm Proteins.** BUNV NSm
475 protein was purified from lysate of the rBUNV-NSmV5 infected cells using anti-V5 Affinity
476 gel (biotool.com). Briefly, BHK-21 cells were infected with rBUNV-NSmV5 and cells were
477 harvested 48 hrs p.i. when cells showed obvious cytopathic effect (CPE). The cell pellet was
478 lysed with non-denaturing RIPA buffer and mixed with anti-V5 Affinity bead. The V5-tagged
479 NSm protein (NSmV5) was separated by 15% Tris-glycine SDS-PAGE (Fig. S3*C*). For
480 preparation of BUNV Gn and Gc proteins, the purified BUNV particles were separated by
481 12.5% Tris-glycine SDS-PAGE and stained with Coomassie Brilliant Blue G-250 solution (Fig.
482 S3*E*). Gn and Gc bands were excised for mass spectrometric analysis.

Mass Spectrometric (MS) Analysis. Protein bands were cut into 1mm cubes, which were then subjected to in-gel digestion with either glutamyl endopeptidase (GluC) (NEB), AspN (NEB) or trypsin (Promega) by a ProGest Investigator in-gel digestion robot (Genomic Solutions, Ann Arbor, MI) using standard protocols (43). Briefly the gel cubes were de-stained by washing with acetonitrile and subjected to reduction and alkylation before digestion with endoproteinase at 37°C. The peptides were then extracted with 10% formic acid and concentrated down to 20 μL using a SpeedVac (ThermoSavant). In some GluC digestions of Gn protein PMSF (1mM) was added to prevent any trypsin-like proteolytic cleavage. The peptides were then separated on an Acclaim PepMap 100 C18 trap and an Acclaim PepMap RSLC C18 column (Thermo Fisher Scientific), using a nanoLC Ultra 2D plus loading pump and nanoLC as-2 autosampler (Eksigent). The peptides were eluted with a gradient of increasing acetonitrile, containing 0.1 % formic acid (5-40% acetonitrile in 5 min, 40-95% in a further 1 min, followed by 95% acetonitrile to clean the column, before reequilibration to 5% acetonitrile). The eluate was sprayed into a TripleTOF 5600+ electrospray tandem mass spectrometer (Sciex) and analyzed in Information Dependent Acquisition (IDA) mode, performing cycles of 250 msec of MS followed by 100 msec MSMS analyses on the 15 most intense peaks seen by MS. The MS/MS data file generated via the 'Create mgf file' script in PeakView (Sciex) was analyzed using the Mascot algorithm (Matrix Science), against an internal database to which the amino acid sequence of the BUNV glycoprotein precursor (Accession number P04505), had been added, with GluC, AspN, or trypsin as the cleavage enzyme and carbamidomethyl as a fixed modification of cysteines and methionine oxidation and deamidation of glutamines and asparagines as a variable modifications, followed by an 'error tolerant' search, to look for peptides where only one end conforms to the enzyme specificity criteria, in order to delineate the C-terminal peptide sequence.

SPP Gene (HM13) Knockdown by Lentivirus shRNA. Short hairpin RNA (shRNA) cDNAs specific for human SPP (nt 777 – 795 for shSPP1 and 1034 – 1052 for shSPP2, Accession No: AJ420895) and eGFP (nt 441 – 463, Accession No: U57607) as control were cloned into pLKO.1 puro (Addgene). Lentivirus stocks were prepared in HEK 293T cells by transfection of constructs: pLKO, pMD-G (pVSVG), a plasmid expressing the vesicular stomatitis virus glycoprotein (VSV-G)(44), and pCMVΔR8.91 (pCMV-R), a plasmid expressing the gag/pol rev genes of HIV-1(45), with Lipofectamine 2000 (Invitrogen). shRNA expression in A549 or A549V cells was achieved by transducing cells with shRNA-expressing lentiviruses for 48 hrs in the presence of 8 µg/ml polybrene (Santa Cruz Biotechnology).

Western Blotting (WB). Lysates of plasmid-transfected or virus-infected cells were prepared by the addition of 100 µl NuPAGE LDS sample buffer (Life Technologies) containing 1µl Benzonase nuclease (Merck Millipore). Proteins were separated on 4 - 12% Bis-Tris protein gel (Life technologies) and transferred to a Nitrocellulose Blotting Membrane (GE Healthcare). The membrane was probed with appropriate antibodies and signals detected by chemiluminescence.

SI Figure Legends

Fig. S1. Schematic of BUNV GPC and mutations at RVAR motif and Amino acid sequence alignment at the BUNV Gn-NSm junction. (*A*) BUNV GPC with positions of amino acid residues marking the predicted boundaries (Gn, NSm and Gc) indicated. The amino acid sequence and the secondary structure prediction at the Gn-NSm junction (residues 295 to 350) are shown below. RVAR motif (residue 299 to 302) is in bold. The epitope to anti-NSm is underlined. The secondary structure is projected using HMMTOP server (http://www.enzim.hu/hmmtop/) with 'H' indicating hydrophobic transmembrane helix, 'i'

532 residue on inside and 'O' residues outside of transmembrane domains (TM/TMD). The NSm
533 domains (I to V) (8) are shown under the NSm coding region. Signal peptide (SP) and TM are
534 shown as grey and black boxes respectively. (*B*) Alignment between BUNV and SSHV GPCs.
535 The previously predicted last C-terminal residues are arginine (R) at residue 302 for BUNV
536 and residue 299 for SSHV (in bold). (*C*) Amino acid sequence alignment of 13
537 orthobunyavirus GPCs (aligned to residues 294 to 335 of BUNV GPC). The alignment was
538 created by using EMBL-EBI Clustal Omega program (www.ebi.ac.uk/Tools/msa/clustalo/).
539 The conserved arginine residues at residue 302 (for BUNV) are in bold. The Accession
540 numbers of orthobunyavirus glycoprotein precursors used in alignment: Bunyamwera virus
541 (BUNV, P04505), Maguari virus (MAGV, AAQ23639), Kairi virus (KRIV, ACV89517), Wyeomyia
542 virus (WYOV, AGA54137), Cachoeira Porteira virus (CPV, AEZ35284), Snowshoe hare virus
543 (SSHV, ABX47014), La Crosse virus (LACV, AAB62804), California encephalitis virus (CEV,
544 AAD53039), Inkoo virus (INKV, AAB93841), Schmallenberg virus (SBV, AGC93514), Douglas
545 virus (DOUV, HE795091), Simbu virus (SIMV, YP_006590085), Oropouche virus (OROV,
546 AGH07923) and Oya virus (OYAV, AGS56983).

547 **Fig. S2.** Effect of Furin inhibitor on BUNV infection. BUNV-infected Vero E6 cells (MOI of
548 0.01 pfu/cell) were incubated for 30 hours in the presence of different concentrations (0,
549 12.5, 25, 50 and 100 µM) of furin inhibitor I (dec-RVKR-cmk, Calbiochem) and viral
550 replication was evaluated by immunoprecipitation and virus titration. (*A*) Effect of the furin
551 inhibitor I on GPC cleavage. Lane 2 is mock infected. (*B*) Yield of virus in the presence of
552 Furin inhibitor I, the concentrations of which are similar to those that inhibit furin-mediated
553 cleavage of the respiratory syncytial virus (RSV) fusion protein (46).

554 **Fig. S3.** Mass spectrometric (MS) analysis of BUNV NSm. (*A*) SP Prediction of NSm domain-I
555 using SignalP 4.1 (www.cbs.dtu.dk/services/SignalP/) (22) with cleavage between residues
556 331G and 332T. (*B*) The V5-tagged NSm (NSmV5). V5 epitope is inserted in the NSm

557 cytoplasmic domain (IV) between residues 403 and 420. (*C*) Purification of NSm from cells
558 infected with recombinant rBUNV-NSmV5. The V5-tagged NSm gel band was excised,
559 subject to in-gel digestion and mass spectrometric analysis. (*D*) MS/MS fragment pattern for
560 the NSm N-terminal residues.

561 **Fig. S4.** Mass spectrometric (MS) analysis of BUNV Gn and Gc. (*A*) Coomassie Blue stained
562 viral proteins of purified virus particles. (*B* to *D*) MS/MS fragment patterns for the terminal
563 residues at Gn N-terminus (*B*) Gn C-terminal region (*C*) and Gc N- terminus (*D*).

564 **Fig. S5. shGFP lentivirus contains antivirus activity.** (*A*) Biological IFN assay. A549/Npro cells
565 were treated with series-diluted IFNα (pbI assay science), lentivirus or cell medium for 24
566 hrs and then challenged with EMCV (at moi of 0.1) for 48 hrs or until obvious CPE occurs.
567 Cells were fixed and stained 4% formaldehyde-0.1% crystal violet solution. (*B*) Comparison
568 of BUNV and PUUV infections responsive to shGFP lentivirus. The induced and naive cells
569 were treated with different dilutions of shGFP lentivirus and infected with either BUNV or
570 PUUV at moi of 0.1. The result was shown as fold inhibition of virus titres between the
571 induced and non-induced cells.

572

573

SI Table. Summary of N- and C-terminal amino acids of Gn, NSm and Gc proteins identified by mass spectrometry.

	Enzyme	Amino acid sequence and position
Gn N-terminal	GluC +PMSF	^{17}SPVITRCFHGGQLIAE
Gn C-terminal	GluC +PMSF	SGLCQGFK ^{296}
		SGLCQGFKS^{297}
		SGLCQGFKSLR^{299}
		SGLCQGFKSLRVAR^{302}
		SGLCQGFKSLRVARR^{303}
	AspN	DRMRMHRESGL^{291}
	Tryp	ESGLCQGFK^{296}
		ESGLCQGFKSLR^{299}
NSm N-terminal	GluC	^{332}TLTNYPTDQK
NSm C-terminal	GluC	CGFCTCGLLEDPEGVVVHK^{441}
Gc N-terminal	Tryp	^{478}EEDCWK
Gc C-terminal	Tryp	LYLQEIK^{1431}

Abbreviation of Endoproteinases: GluC, Glutamyl endopeptidase; AspN, Peptidyl-Asp metalloendopeptidase, Tryp, trypsin.

REFERENCES

1. Plyusnin A & Elliott RM eds (2011) *Bunyaviridae*. *Molecular and Cellular Biology* (Caister Academic Press, Norfolk).

584 2. Elliott RM & Schmaljohn CS (2013) Bunyaviridae. *Fields Virology*, eds Knipe DM
585 & Howley PM (Wolters Kluwer, Philadelphia), 6 Ed, pp 1244-1282.

586 3. Shi X, van Mierlo JT, French A, & Elliott RM (2010) Visualizing the Replication
587 Cycle of Bunyamwera Orthobunyavirus Expressing Fluorescent Protein-Tagged Gc
588 Glycoprotein. *J. Virol.* 84(17):8460-8469.

589 4. Shi X, Brauburger K, & Elliott RM (2005) Role of N-linked glycans on Bunyamwera
590 virus glycoproteins in intracellular trafficking, protein folding, and virus infectivity.
591 *J. Virol.* 79(21):13725-13734.

592 5. Bowden TA, *et al.* (2013) Orthobunyavirus ultrastructure and the curious tripodal
593 glycoprotein spike. *PLos Pathogens* 9(5):e1003374.

594 6. Garry CE & Garry RF (2004) Proteomics computational analyses suggest that the
595 carboxyl terminal glycoproteins of Bunyaviruses are class II viral fusion protein
596 (beta-penetrenes). *Theor Biol Med Model* 1:10.

597 7. Shi X, Kohl A, Li P, & Elliott RM (2007) Role of the cytoplasmic tail domains of
598 Bunyamwera orthobunyavirus glycoproteins Gn and Gc in virus assembly and
599 morphogenesis. *J. Virol.* 81(18):10151-10160.

600 8. Shi X, *et al.* (2006) Requirement of the N-terminal region of the orthobunyavirus
601 non-structural protein NSm for virus assembly and morphogenesis. *J Virol*
602 80(16):8089-8099.

603 9. Fazakerley JK, *et al.* (1988) Organization of the middle RNA segment of snowshoe
604 hare Bunyavirus. *Virology* 167(2):422-432.

605 10. Briese T, Rambaut A, & Lipkin WI (2004) Analysis of the medium (M) segment
606 sequence of Guaroa virus and its comparison to other orthobunyaviruses. *J Gen Virol*
607 85(Pt 10):3071-3077.

608 11. Elliott RM & Blakqori G (2011) Molecuar biology of Orthobunyaviruses.
609 *Bunyaviridae*, eds Plyusnin A & Elliot RM (Causter Academic Press, Norfork, UK),
610 p 1 to 39.

611 12. Auclair SM, Bhanu MK, & Kendall DA (2012) Signal peptidase I: Cleaving the way
612 to mature proteins. *Protein Science* 21(1):13-25.

613 13. Golde TE, Wolfe MS, & Greenbaum DC (2009) Signal peptide peptidases: A family
614 of intramembrane-cleaving proteases that cleave type 2 transmembrane proteins.
615 *Seminars in Cell & Developmental Biology* 20(2):225-230.

616 14. Lemberg MK (2011) Intramembrane Proteolysis in Regulated Protein Trafficking.
617 *Traffic* 12(9):1109-1118.

618 15. Voss M, Schr√ ∂ der B, & Fluhrer R (2013) Mechanism, specificity, and physiology
619 of signal peptide peptidase (SPP) and SPP-like proteases. *Biochimica et Biophysica*
620 *Acta (BBA) - Biomembranes* 1828(12):2828-2839.

16. Weihofen A & Martoglio B (2003) Intramembrane-cleaving proteases: controlled liberation of proteins and bioactive peptides. *Trends in Cell Biology* 13(2):71-78.

17. Friedmann E*, et al.* (2006) SPPL2a and SPPL2b promote intramembrane proteolysis of TNF[alpha] in activated dendritic cells to trigger IL-12 production. *Nat Cell Biol* 8(8):843-848.

18. Oliveira CuC*, et al.* (2013) New Role of Signal Peptide Peptidase To Liberate C-Terminal Peptides for MHC Class I Presentation. *The Journal of Immunology* 191(8):4020-4028.

19. Lemberg MK, Bland FA, Weihofen A, Braud VM, & Martoglio B (2001) Intramembrane Proteolysis of Signal Peptides: An Essential Step in the Generation of HLA-E Epitopes. *The Journal of Immunology* 167(11):6441-6446.

20. McLauchlan J, Lemberg MK, Hope G, & Martoglio B (2002) Intramembrane proteolysis promotes trafficking of hepatitis C virus core protein to lipid droplets. *Embo J* 21(15):3980-3988.

21. Bintintan I & Meyers G (2010) A New Type of Signal Peptidase Cleavage Site Identified in an RNA Virus Polyprotein. *Journal of Biological Chemistry* 285(12):8572-8584.

22. Petersen TN, Brunak S, von Heijne G, & Nielsen H (2011) SignalP 4.0: discriminating signal peptides from transmembrane regions. *Nat Methods* 8(10):785-786.

23. von Heijne G (1986) A new method for predicting signal sequence cleavage sites. *Nucleic Acids Research* 14(11):4683-4690.

24. Evnin LB, Vásquez JR, & Craik CS (1990) Substrate specificity of trypsin investigated by using a genetic selection. *Proceedings of the National Academy of Sciences* 87(17):6659-6663.

25. Fontana J, LÛpez-Montero N, Elliott RM, Fern·ndez JJs, & Risco C (2008) The unique architecture of Bunyamwera virus factories around the Golgi complex. *Cellular Microbiology* 10(10):2012-2028.

26. Lappin DF, Nakitare GW, Palfreyman JW, & Elliott RM (1994) Localization of Bunyamwera bunyavirus G1 glycoprotein to the Golgi requires association with G2 but not with NSm. *J Gen Virol* 75:3441-3451.

27. Tilston-Lunel NL, Acrani GO, Randall RE, & Elliott RM (2016) Generation of Recombinant Oropouche Viruses Lacking the Nonstructural Protein NSm or NSs. *Journal of Virology* 90(5):2616-2627.

28. Thomas G (2002) Furin at the cutting edge: from protein traffic to embryogenesis and disease. *Nature reviews. Molecular cell biology* 3(10):753-766.

29. Seidah NG & Prat A (2012) The biology and therapeutic targeting of the proprotein convertases. *Nat Rev Drug Discov* 11(5):367-383.

30. Sanchez AJ, Vincent MJ, Erickson BR, & Nichol ST (2006) Crimean-Congo Hemorrhagic Fever Virus Glycoprotein Precursor Is Cleaved by Furin-Like and SKI-1 Proteases To Generate a Novel 38-Kilodalton Glycoprotein. *Journal of Virololgy* 80:514-525.

31. Bridge AJ, Pebernard S, Ducraux A, Nicoulaz AL, & Iggo R (2003) Induction of an interferon response by RNAi vectors in mammalian cells. *Nat Genet* 34(3):263-264.

32. Whitehead KA, Dahlman JE, Langer RS, & Anderson DG (2011) Silencing or Stimulation? siRNA Delivery and the Immune System. *Annual Review of Chemical and Biomolecular Engineering* 2(1):77-96.

33. Schrempf S, Froeschke M, Giroglou T, von Laer D, & Dobberstein B (2007) Signal Peptide Requirements for Lymphocytic Choriomeningitis Virus Glycoprotein C Maturation and Virus Infectivity. *Journal of Virology* 81(22):12515-12524.

34. Bederka LH, Bonhomme CJ, Ling EL, & Buchmeier MJ (2014) Arenavirus Stable Signal Peptide Is the Keystone Subunit for Glycoprotein Complex Organization. *mBio* 5(6).

35. York J, Romanowski V, Lu M, & Nunberg JH (2004) The Signal Peptide of the Junín Arenavirus Envelope Glycoprotein Is Myristoylated and Forms an Essential Subunit of the Mature G1-G2 Complex. *Journal of Virology* 78(19):10783-10792.

36. Killip MJ, *et al.* (2013) Deep Sequencing Analysis of Defective Genomes of Parainfluenza Virus 5 and Their Role in Interferon Induction. *Journal of Virology* 87(9):4798-4807.

37. Hale BG, *et al.* (2009) CDK/ERK-mediated phosphorylation of the human influenza A virus NS1 protein at threonine-215. *Virology* 383(1):6-11.

38. Buchholz UJ, Finke S, & Conzelmann KK (1999) Generation of bovine respiratory syncytial virus (BRSV) from cDNA: BRSV NS2 is not essential for virus replication in tissue culture, and the human RSV leader region acts as a functional BRSV genome promoter. *J Virol* 73(1):251-259.

39. Weber F, Dunn EF, Bridgen A, & Elliott RM (2001) The Bunyamwera virus nonstructural protein NSs inhibits viral RNA synthesis in a minireplicon system. *Virology* 281(1):67-74.

40. Elliott RM, *et al.* (2013) Establishment of a reverse genetics system for Schmallenberg virus, a newly emerged orthobunyavirus in Europe. *Journal of General Virology* 94(Pt 4):851-859.

41. Brennan B, Li P, & Elliott RM (2011) Generation and characterization of a recombinant Rift Valley fever virus expressing a V5 epitope-tagged RNA-dependent RNA polymerase. *Journal of General Virology* 92(12):2906-2913.

42. Lowen AC, Noonan C, McLees A, & Elliott RM (2004) Efficient bunyavirus rescue from cloned cDNA. *Virology* 330(2):493-500.

43. Shevchenko A, Wilm M, Vorm O, & Mann M (1996) Mass spectrometric sequencing of proteins silver-stained polyacrylamide gels. *Analytical Chemistry* 68(5):850-858.

44. Naldini L, Blömer U, Gage FH, Trono D, & Verma IM (1996) Efficient transfer, integration, and sustained long-term expression of the transgene in adult rat brains injected with a lentiviral vector. *Proceedings of the National Academy of Sciences* 93(21):11382-11388.

45. Zufferey R, Nagy D, Mandel RJ, Naldini L, & Trono D (1997) Multiply attenuated lentiviral vector achieves efficient gene delivery in vivo. *Nat Biotechnol* 15(9):871-875.

46. Sugrue RJ, Brown C, Brown G, Aitken J, & McL. Rixon HW (2001) Furin cleavage of the respiratory syncytial virus fusion protein is not a requirement for its transport to the surface of virus-infected cells. *Journal of General Virology* 82(6):1375-1386.

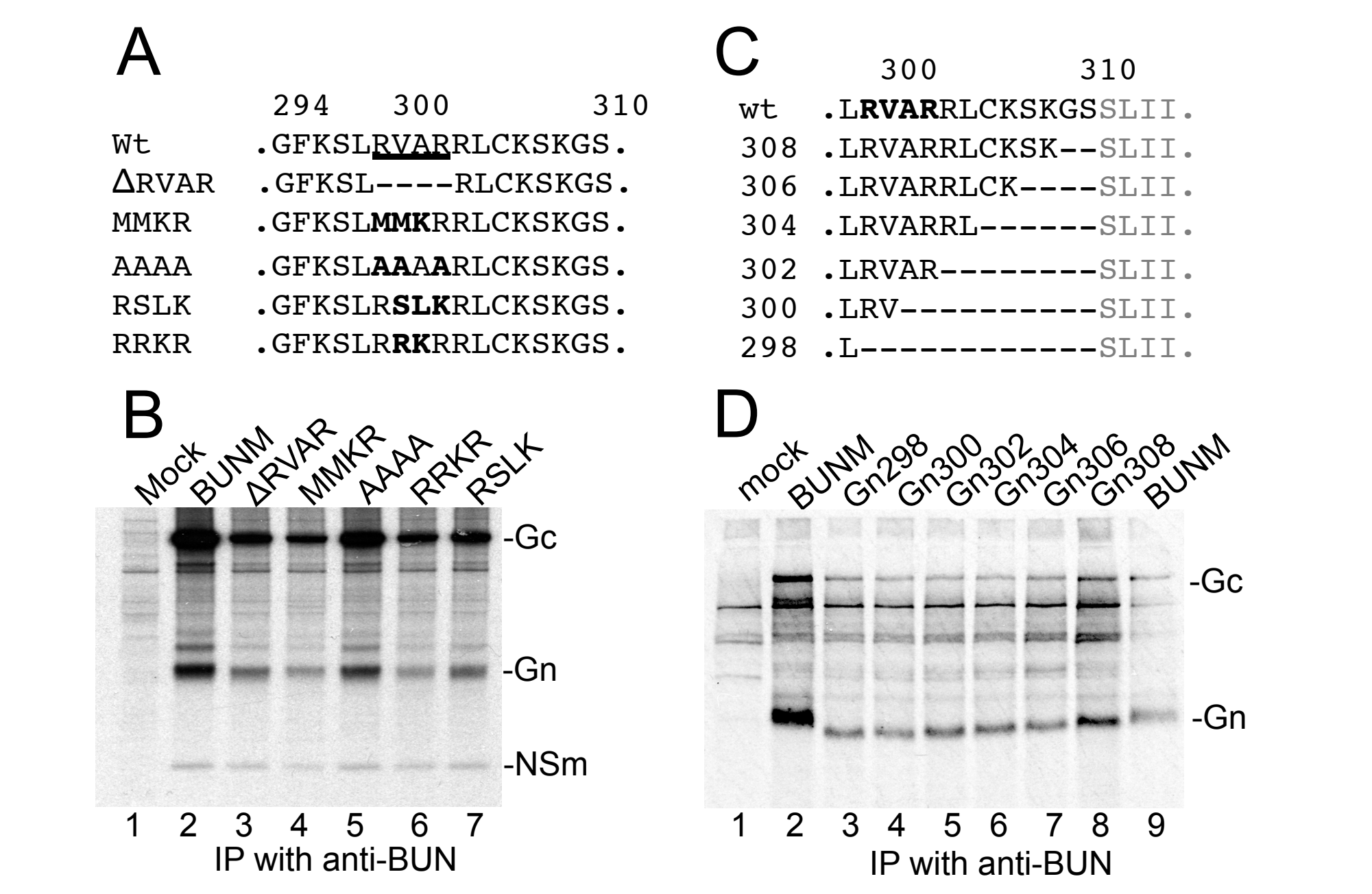
A
294 300 310
Wt .GFKSLRVARRLCKSKGS.
ΔRVAR .GFKSL----RLCKSKGS.
MMKR .GFKSLMMKRRLCKSKGS.
AAAA .GFKSLAAAARLCKSKGS.
RSLK .GFKSLRSLKRLCKSKGS.
RRKR .GFKSLRRKRRLCKSKGS.
C
300 310
wt .LRVARRLCKSKGSSLII.
308 .LRVARRLCKSK--SLII.
306 .LRVARRLCK----SLII.
304 .LRVARRL------SLII.
302 .LRVAR--------SLII.
300 .LRV----------SLII.
298 .L-----------SLII.
B
Mock
BUNM
ΔRVAR
MMKR
AAAA
RRKR
RSLK
-Gc
-Gn
-NSm
1 2 3 4 5 6 7
IP with anti-BUN
D
mock
BUNM
Gn298
Gn300
Gn302
Gn304
Gn306
Gn308
BUNM
-Gc
-Gn
1 2 3 4 5 6 7 8 9
IP with anti-BUN

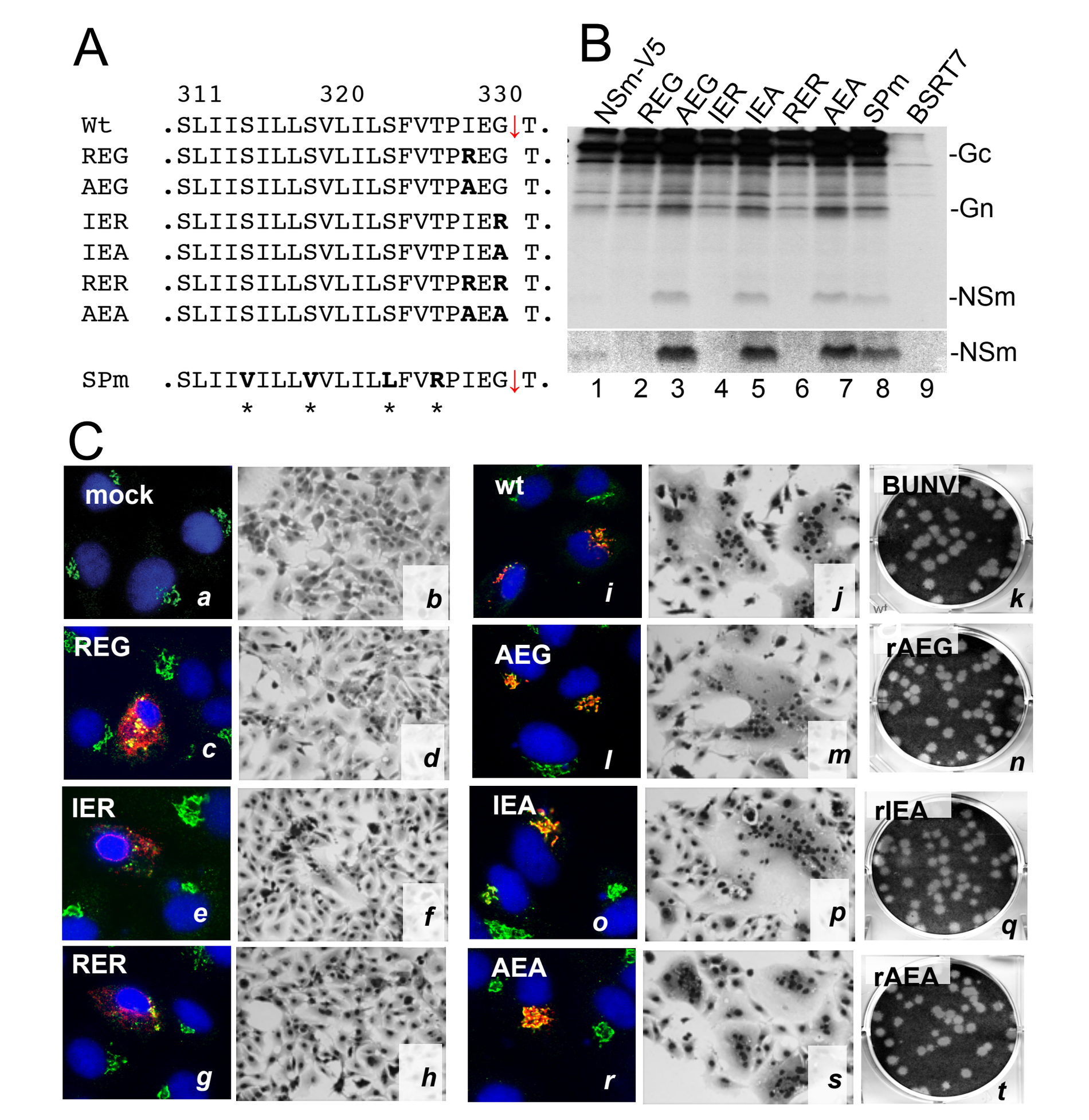
A
311
320
330
Wt .SLIISILLSVLILSFVTPIEG↓T.
REG .SLIISILLSVLILSFVTPREG T.
AEG .SLIISILLSVLILSFVTPAEG T.
IER .SLIISILLSVLILSFVTPIER T.
IEA .SLIISILLSVLILSFVTPIEA T.
RER .SLIISILLSVLILSFVTPRER T.
AEA .SLIISILLSVLILSFVTPAEA T.
SPm .SLIIVILLVVLILLFVRPIEG↓T.
* * * *
B
NSm-V5
REG
AEG
IER
IEA
RER
AEA
SPm
BSRT7
-Gc
-Gn
-NSm
-NSm
1 2 3 4 5 6 7 8 9
C
mock
a
b
wt
i
j
BUNV
k
REG
c
d
AEG
l
m
rAEG
n
IER
e
f
IEA
o
p
rIEA
q
RER
g
h
AEA
r
s
rAEA
t

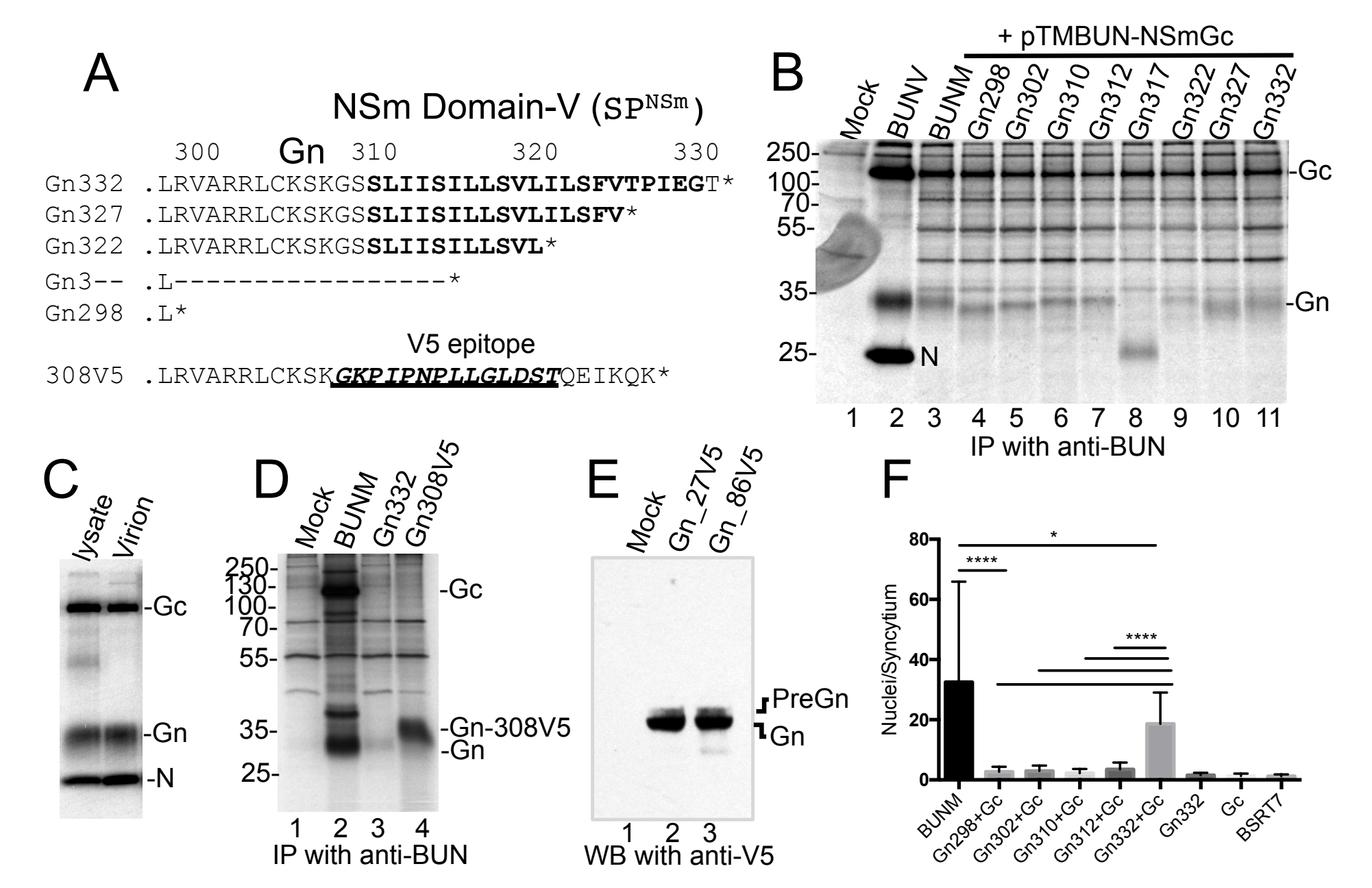
A
NSm Domain-V (SP^NSm)
300
Gn
310
320
330
Gn332 .LRVARRLCKSKGSSLIISILLSVLILSFVTPIEGT*
Gn327 .LRVARRLCKSKGSSLIISILLSVLILSFV*
Gn322 .LRVARRLCKSKGSSLIISILLSVL*
Gn3-- .L----------*
Gn298 .L*
V5 epitope
308V5 .LRVARRLCKSKGKPIPNPLLGLDSTQEIKQK*
B
+ pTMBUN-NSmGc
Mock
BUNV
BUNM
Gn298
Gn302
Gn310
Gn312
Gn317
Gn322
Gn327
Gn332
250-
100-
70-
55-
35-
25-
-Gc
-Gn
N
1 2 3 4 5 6 7 8 9 10 11
IP with anti-BUN
C
lysate
Virion
-Gc
-Gn
-N
D
Mock
BUNM
Gn332
Gn308V5
250-
130-
100-
70-
55-
35-
25-
-Gc
-Gn-308V5
-Gn
1 2 3 4
IP with anti-BUN
E
Mock
Gn_27V5
Gn_86V5
PreGn
Gn
1 2 3
WB with anti-V5
F
Nuclei/Syncytium
80
60
40
20
0
*
****
****
BUNM
Gn298+Gc
Gn302+Gc
Gn310+Gc
Gn312+Gc
Gn332+Gc
Gn332
Gc
BSRT7

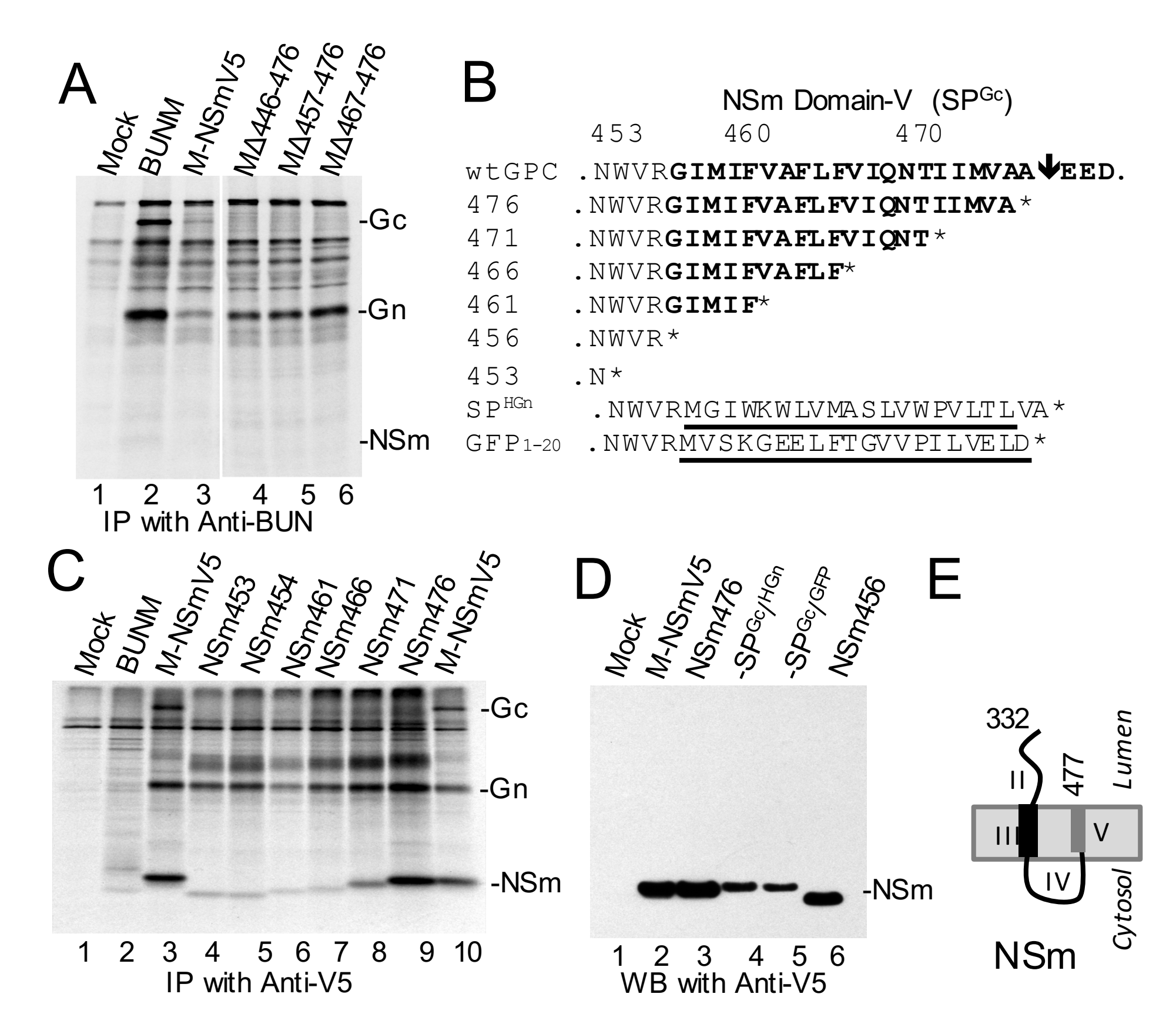
A
Mock
BUNM
M-NSmV5
MΔ446-476
MΔ457-476
MΔ467-476
-Gc
-Gn
-NSm
1 2 3 4 5 6
IP with Anti-BUN
B
NSm Domain-V (SPGc)
453 460 470
wtGPC .NWVRGIMIFVAFLFVIQNTIIMVAA↓EED.
476 .NWVRGIMIFVAFLFVIQNTIIMVA*
471 .NWVRGIMIFVAFLFVIQNT*
466 .NWVRGIMIFVAFLF*
461 .NWVRGIMIF*
456 .NWVR*
453 .N*
SPHGn .NWVRMGIWKWLVMASLVWPVLTLVA*
GFP1-20 .NWVRMVSKGEELFTGVVPILVELD*
C
Mock
BUNM
M-NSmV5
NSm453
NSm454
NSm461
NSm466
NSm471
NSm476
M-NSmV5
-Gc
-Gn
-NSm
1 2 3 4 5 6 7 8 9 10
IP with Anti-V5
D
Mock
M-NSmV5
NSm476
-SPGc/HGn
-SPGc/GFP
NSm456
-NSm
1 2 3 4 5 6
WB with Anti-V5
E
332
II
477
Lumen
III
V
IV
Cytosol
NSm

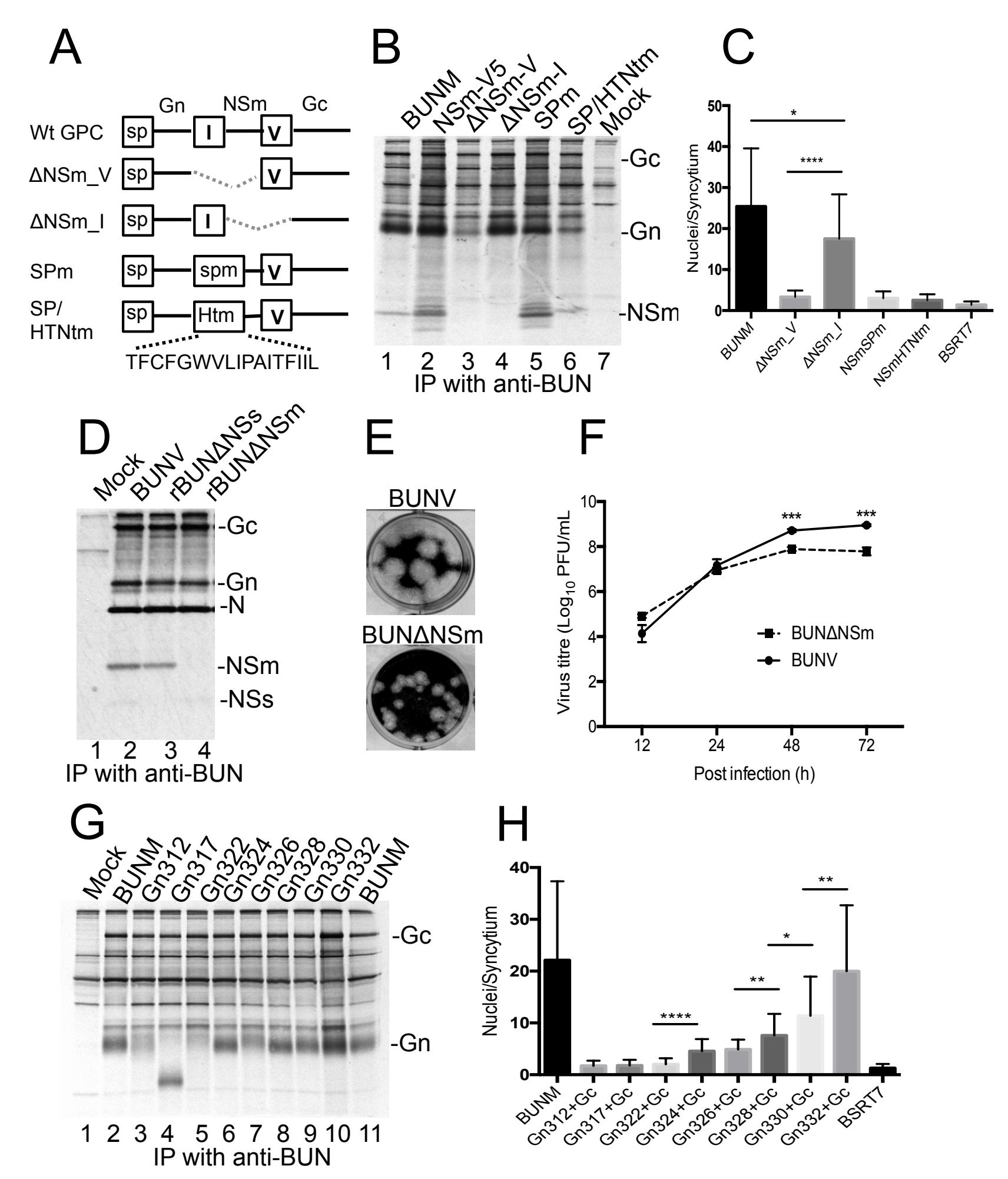
A
Gn
NSm
Gc
Wt GPC
sp
I
V
ΔNSm_V
ΔNSm_I
SPm
spm
SP/
HTNtm
Htm
TFCFGWVLIPAITFIIL
B
BUNM
NSm-V5
ΔNSm-V
ΔNSm-I
SPm
SP/HTNtm
Mock
-Gc
-Gn
-NSm
1 2 3 4 5 6 7
IP with anti-BUN
C
Nuclei/Syncytium
50
40
30
20
10
0
*
****
BUNM
ΔNSm_V
ΔNSm_I
NSmSPm
NSmHTNtm
BSRT7
D
Mock
BUNV
rBUNΔNSs
rBUNΔNSm
-Gc
-Gn
-N
-NSm
-NSs
1 2 3 4
IP with anti-BUN
E
BUNV
BUNΔNSm
F
Virus titre (Log10 PFU/mL
10
8
6
4
2
0
***
***
BUNΔNSm
BUNV
12
24
48
72
Post infection (h)
G
Mock
BUNM
Gn312
Gn317
Gn322
Gn324
Gn326
Gn328
Gn330
Gn332
BUNM
-Gc
-Gn
1 2 3 4 5 6 7 8 9 10 11
IP with anti-BUN
H
Nuclei/Syncytium
40
30
20
10
0
****
**
*
**
BUNM
Gn312+Gc
Gn317+Gc
Gn322+Gc
Gn324+Gc
Gn326+Gc
Gn328+Gc
Gn330+Gc
Gn332+Gc
BSRT7

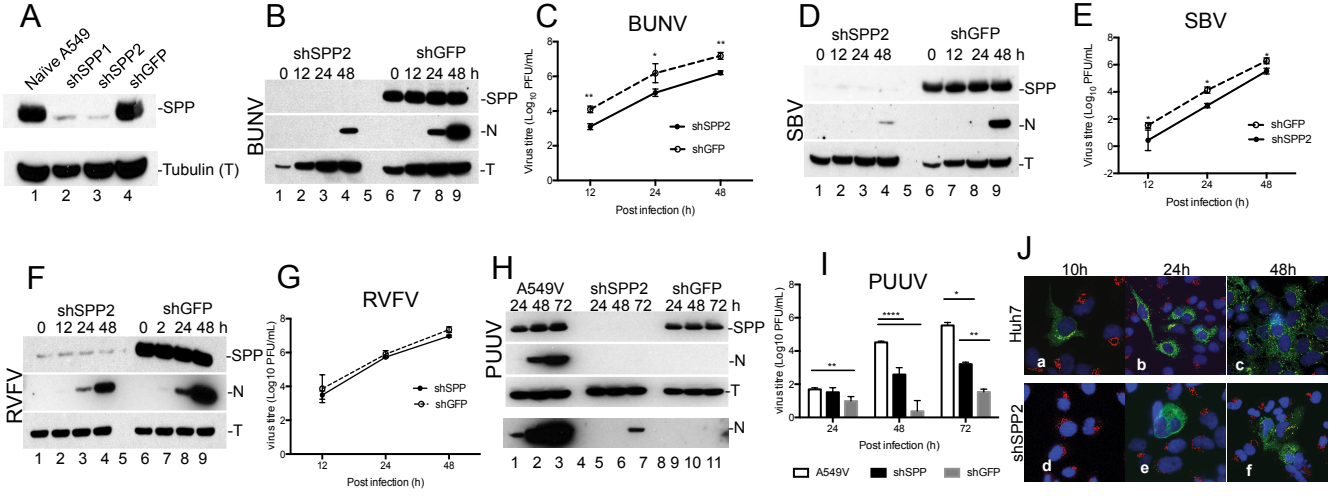
A
Naive A549
shSPP1
shSPP2
shGFP
-SPP
-Tubulin (T)
1 2 3 4
B
shSPP2
shGFP
0 12 24 48
0 12 24 48 h
BUNV
-SPP
-N
-T
1 2 3 4 5 6 7 8 9
C
BUNV
Virus titre (Log10 PFU/mL
shSPP2
shGFP
Post infection (h)
D
shSPP2
shGFP
0 12 24 48
0 12 24 48 h
SBV
-SPP
-N
-T
1 2 3 4 5 6 7 8 9
E
SBV
Virus titre (Log10 PFU/mL
shGFP
shSPP2
Post infection (h)
F
shSPP2
shGFP
0 12 24 48
0 2 24 48 h
RVFV
-SPP
-N
-T
1 2 3 4 5 6 7 8 9
G
RVFV
virus titre (Log10 PFU/mL)
shSPP
shGFP
Post infection (h)
H
A549V
shSPP2
shGFP
24 48 72
24 48 72
24 48 72 h
PUUV
-SPP
-N
-T
-N
1 2 3 4 5 6 7 8 9 10 11
I
PUUV
virus titre (Log10 PFU/mL)
Post infection (h)
A549V
shSPP
shGFP
J
10h
24h
48h
Huh7
shSPP2
a
b
c
d
e
f

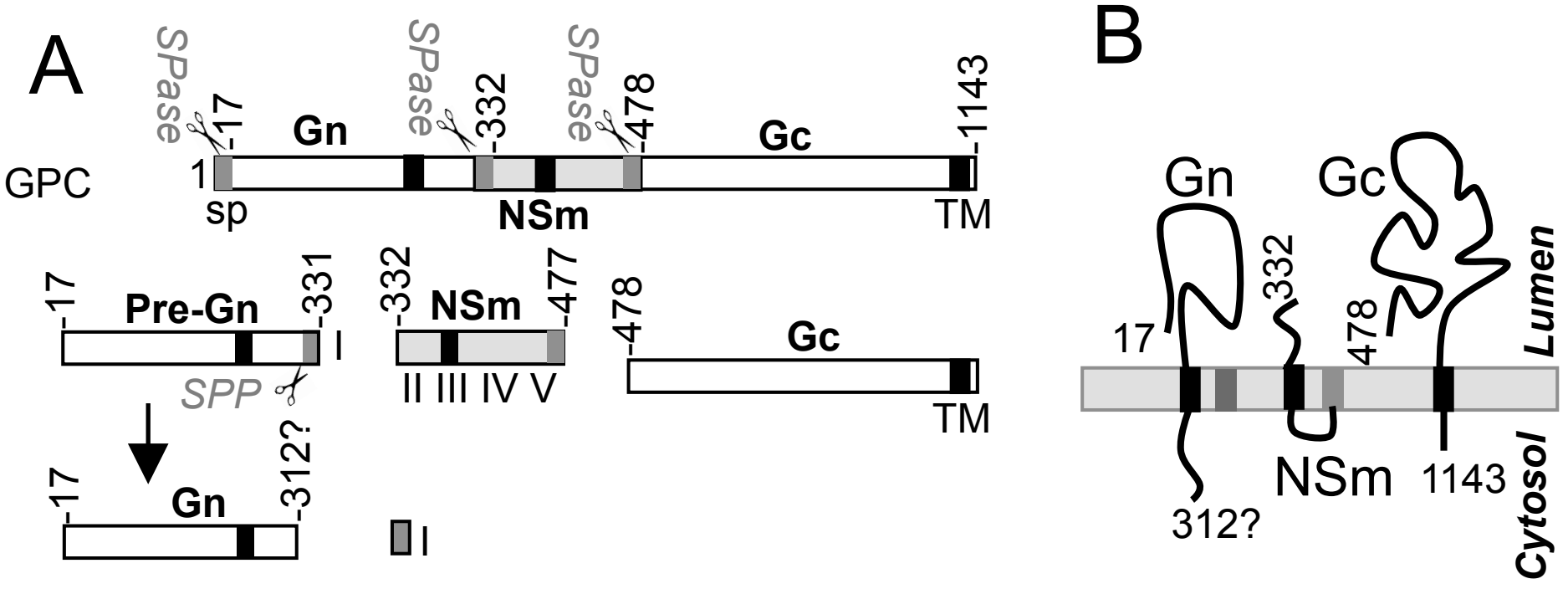
A
SPase
SPase
SPase
-17
-332
-478
-1143
Gn
Gc
GPC
1
sp
NSm
TM
-17
Pre-Gn
-331
-332
NSm
-477
-478
Gc
SPP
II III IV V
TM
-17
Gn
-312?
B
Gn
Gc
17
332
478
Lumen
NSm
1143
312?
Cytosol

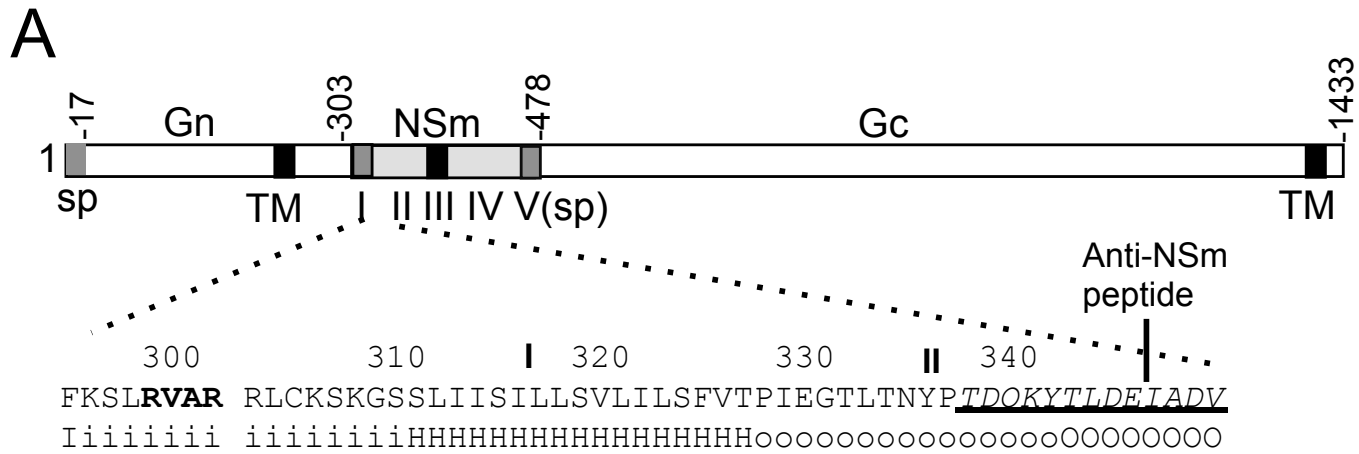
A
-17
Gn
-303
NSm
-478
Gc
-1433
1
sp
TM
I II III IV V(sp)
TM
Anti-NSm
peptide
300 310 I 320 330 II 340
FKSLRVAR RLCKSKGSSLIISILLSVLILSFVTPIEGTLTNYPTDQKYTLDEIADV
Iiiiiiii iiiiiiiiHHHHHHHHHHHHHHHHHHoooooooooooooooOOOOOOOO

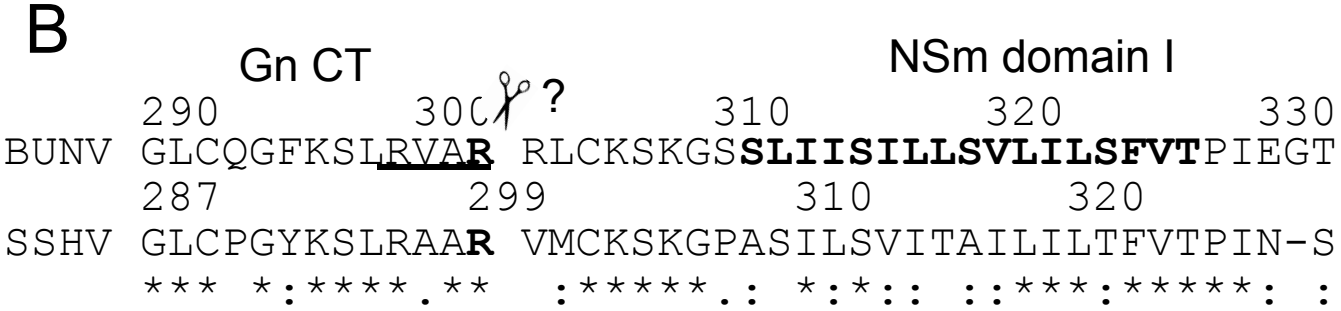
B
Gn CT
NSm domain I
290 300 ? 310 320 330
BUNV GLCQGFKSLRVAR RLCKSKGSSLIISILLSVLILSFVTPIEGT
287 299 310 320
SSHV GLCPGYKSLRAAR VMCKSKGPASILSVITAILILTFVTPIN-S

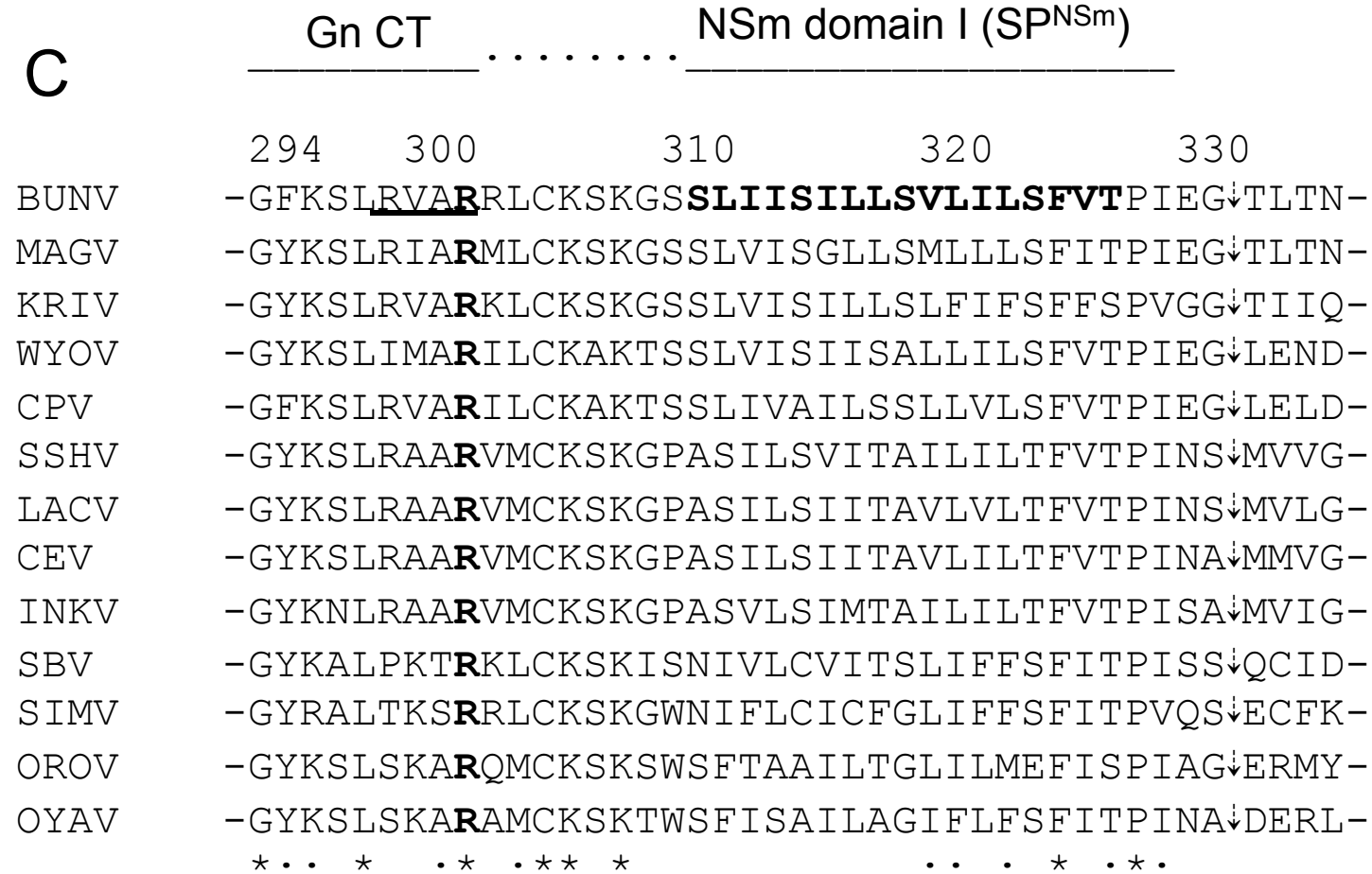
C
Gn CT
NSm domain I (SPNSm)
294 300 310 320 330
BUNV -GFKSLRVARRLCKSKGSSLIISILLSVLILSFVTPIEG↓TLTN-
MAGV -GYKSLRIARMLCKSKGSSLVISGLLSMLLLSFITPIEG↓TLTN-
KRIV -GYKSLRVARKLCKSKGSSLVISILLSLFIFSFFSPVGG↓TIIQ-
WYOV -GYKSLIMARILCKAKTSSLVISIISALLILSFVTPIEG↓LEND-
CPV -GFKSLRVARILCKAKTSSLIVAILSSLLVLSFVTPIEG↓LELD-
SSHV -GYKSLRAARVMCKSKGPASILSVITAILILTFVTPINS↓MVVG-
LACV -GYKSLRAARVMCKSKGPASILSIITAVLVLTFVTPINS↓MVLG-
CEV -GYKSLRAARVMCKSKGPASILSIITAVLILTFVTPINA↓MMVG-
INKV -GYKNLRAARVMCKSKGPASVLSIMTAILILTFVTPISA↓MVIG-
SBV -GYKALPKTRKLCKSKISNIVLCVITSLIFFSFITPISS↓QCID-
SIMV -GYRALTKSRRLCKSKGWNIFLCICFGLIFFSFITPVQS↓ECFK-
OROV -GYKSLSKARQMCKSKSWSFTAAILTGLILMEFISPIAG↓ERMY-
OYAV -GYKSLSKARAMCKSKTWSFISAILAGIFLFSFITPINA↓DERL-

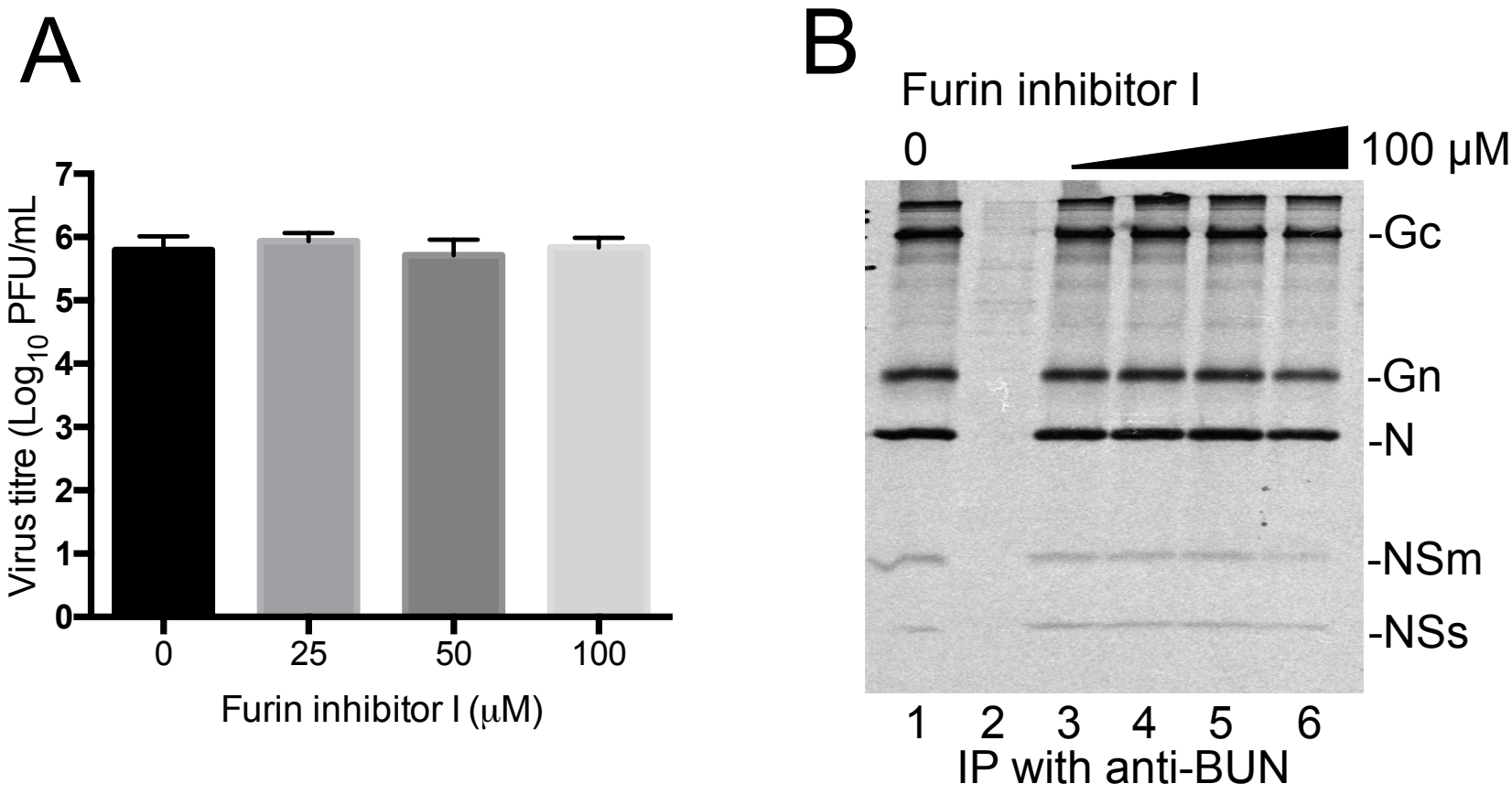
A
Virus titre (Log10 PFU/mL
0
1
2
3
4
5
6
7
0
25
50
100
Furin inhibitor I (μM)
B
Furin inhibitor I
0
100 μM
-Gc
-Gn
-N
-NSm
-NSs
1
2
3
4
5
6
IP with anti-BUN

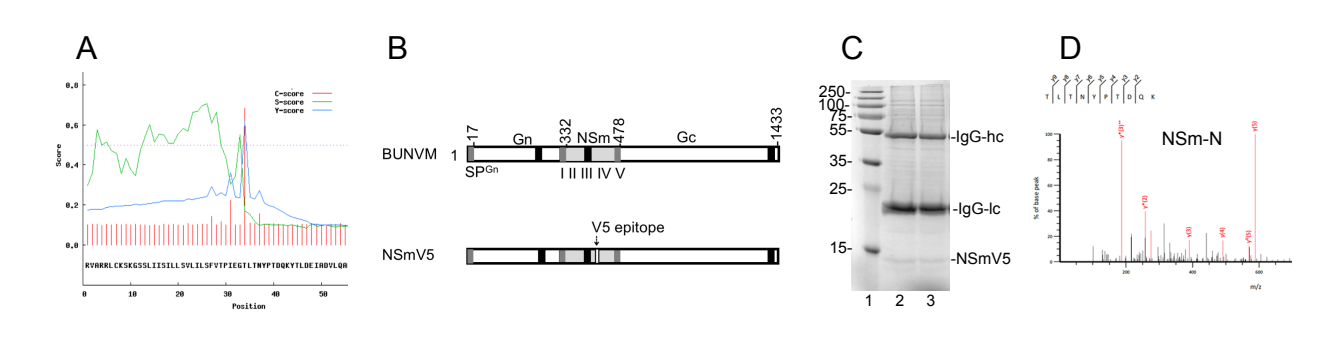
A
C-score
S-score
Y-score
Score
RVARRLCKSKGSSLIISILLSVLILSFVTPIEGTLTNYPTDQKYTLDEIADVLQR
Position
B
BUNVM
1
17
Gn
332
NSm
478
Gc
1433
SPGn
I II III IV V
V5 epitope
NSmV5
C
250-
100-
75-
55-
35-
25-
15-
IgG-hc
IgG-lc
NSmV5
1 2 3
D
T L T N Y P T D Q K
NSm-N
% of base peak
m/z

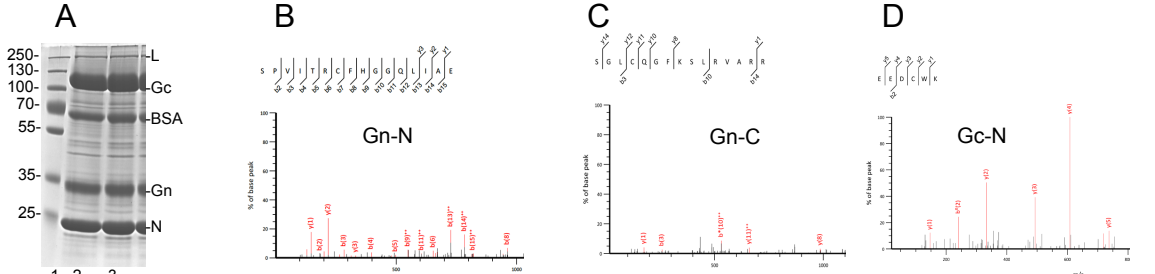
A
250-
130-
100-
70-
55-
35-
25-
L
Gc
BSA
Gn
N
1 2 3
B
Gn-N
% of base peak
m/z
C
Gn-C
% of base peak
m/z
D
Gc-N
% of base peak
m/z

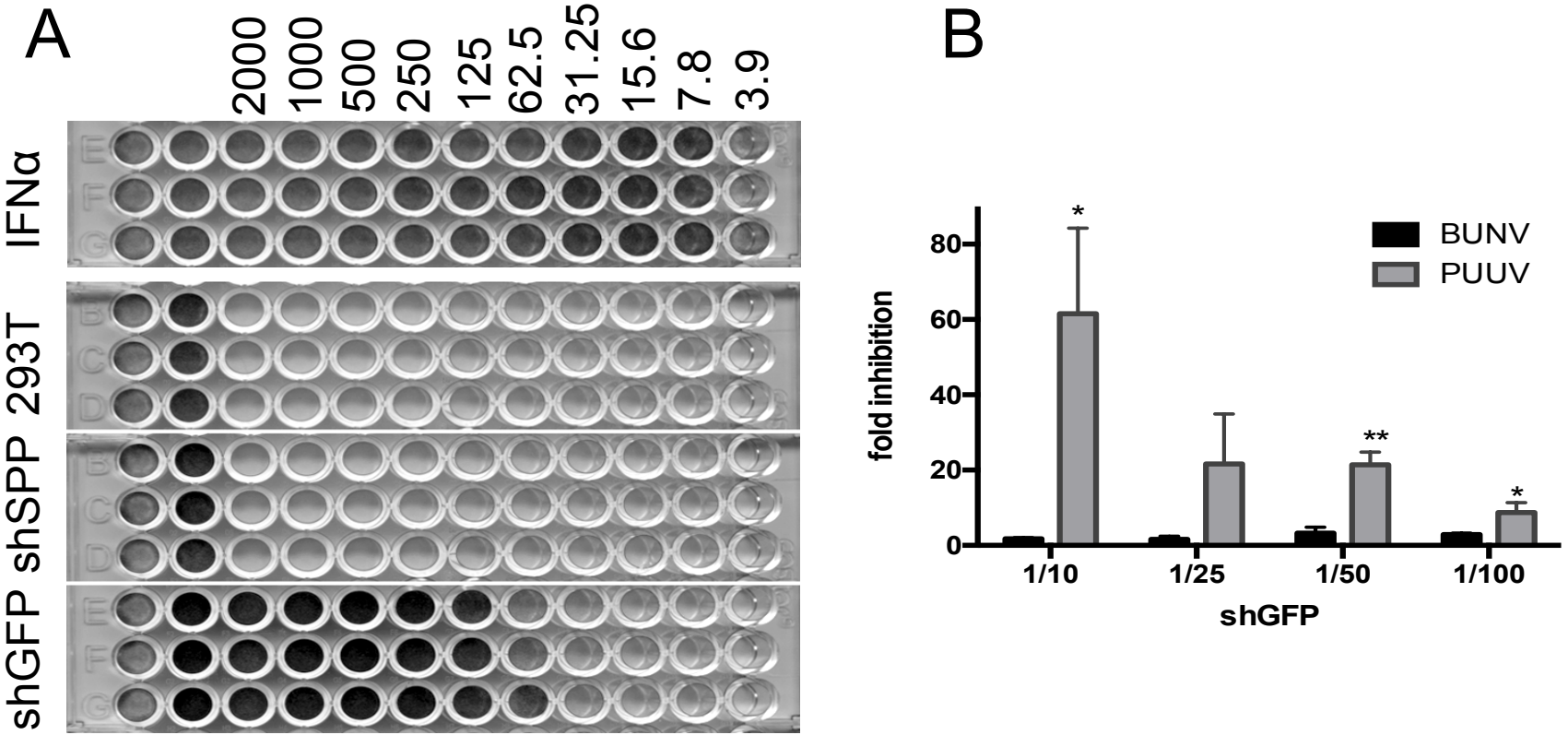
A
2000
1000
500
250
125
62.5
31.25
15.6
7.8
3.9
IFNα
293T
shSPP
shGFP
B
fold inhibition
80
60
40
20
0
*
**
*
BUNV
PUUV
1/10
1/25
1/50
1/100
shGFP